



# COMPOSITIO MATHEMATICA

## Hamiltonian knottedness and lifting paths from the shape invariant

Richard Hind and Jun Zhang

Compositio Math. **159** (2023), 2416–2457.

[doi:10.1112/S0010437X23007479](https://doi.org/10.1112/S0010437X23007479)





# Hamiltonian knottedness and lifting paths from the shape invariant

Richard Hind and Jun Zhang

## ABSTRACT

The Hamiltonian shape invariant of a domain  $X \subset \mathbb{R}^4$ , as a subset of  $\mathbb{R}^2$ , describes the product Lagrangian tori which may be embedded in  $X$ . We provide necessary and sufficient conditions to determine whether or not a path in the shape invariant can lift, that is, be realized as a smooth family of embedded Lagrangian tori, when  $X$  is a basic 4-dimensional toric domain such as a ball  $B^4(R)$ , an ellipsoid  $E(a, b)$  with  $b/a \in \mathbb{N}_{\geq 2}$ , or a polydisk  $P(c, d)$ . As applications, via the path lifting, we can detect knotted embeddings of product Lagrangian tori in many toric  $X$ . We also obtain novel obstructions to symplectic embeddings between domains that are more general than toric concave or toric convex.

## 1. Notation

Here we gather some common notation. We work in  $\mathbb{R}^4 \equiv \mathbb{C}^2$  with the standard symplectic form  $\omega = (i/2) \sum_{k=1}^2 dz_k \wedge d\bar{z}_k$ . The moment map is

$$\mu : \mathbb{C}^2 \rightarrow \mathbb{R}_{\geq 0}^2 \quad (z_1, z_2) \mapsto (\pi|z_1|^2, \pi|z_2|^2).$$

We use coordinates  $(r, s)$  on  $\mathbb{R}_{\geq 0}^2$ . Given a subset  $\Omega \subset \mathbb{R}_{\geq 0}^2$  we define the corresponding toric domain  $X_\Omega := \mu^{-1}(\Omega) \subset \mathbb{C}^2$ . A toric *star-shaped* domain  $X_\Omega$  has  $\partial\Omega$  transversal to the radial vector field  $X_{\text{rad}} = r(\partial/\partial r) + s(\partial/\partial s)$  of  $\mathbb{R}_{>0}^2$ . In the case when this subset  $\Omega$  is of the form

$$\Omega = \{(r, s) \in \mathbb{R}^2 \mid 0 \leq r \leq a, 0 \leq s \leq f(r)\},$$

we say that  $X_\Omega$  is (toric) *convex* if  $f$  is concave, and  $X_\Omega$  is (toric) *concave* if  $f$  is convex. Examples of toric domains which are both convex and concave are symplectic (closed) ellipsoids. We define the (open) ellipsoid  $E(a, b) := X_{\Delta(a,b)}$  with  $0 < a \leq b$ , where  $\Delta(a, b) := \{0 \leq r < a, 0 \leq s < b - br/a\}$ . The ball of capacity  $R$  is denoted by  $B^4(R) = E(R, R)$ . We say that an ellipsoid  $E(a, b)$  is *integral* if  $b/a \in \mathbb{N}_{\geq 2}$ . The polydisk  $P(c, d) := X_{\square(c,d)}$  with  $0 < c \leq d$ , where  $\square(a, b) := \{0 \leq r < a, 0 \leq s < b\}$ . A product Lagrangian torus is a torus

$$L(r, s) := X_{\{(r,s)\}} = \mu^{-1}(r, s). \tag{1}$$

Received 15 September 2021, accepted in final form 17 May 2023, published online 18 September 2023.

2020 Mathematics Subject Classification 53D12 (primary), 53D35 (secondary).

Keywords: Lagrangian tori, shape invariant, Hamiltonian knottedness, symplectic embedding.

The first named author is supported by Simons Foundation Grant no. 633715. The second named author is currently supported by USTC Research Funds of the Double First-Class Initiative.

© 2023 The Author(s). This is an Open Access article, distributed under the terms of the Creative Commons Attribution-NonCommercial licence (<https://creativecommons.org/licenses/by/4.0>), which permits noncommercial re-use, distribution, and reproduction in any medium, provided the original article is properly cited. Written permission must be obtained prior to any commercial use. *Compositio Mathematica* is © Foundation Compositio Mathematica.

Given subsets  $U, V \subset \mathbb{R}^4$  we write  $\Phi : U \hookrightarrow V$  to mean that there exists a Hamiltonian diffeomorphism  $\Phi$  of  $\mathbb{R}^4$  embedding  $U$  into  $\text{int}(V)$ . If  $\Phi$  is not emphasized, we simply denote such an embedding by  $U \hookrightarrow V$ .

We will denote by  $\mathcal{L}(X)$  the set of Lagrangian tori in a domain  $X \subset \mathbb{C}^2$  which are Hamiltonian isotopic in  $\mathbb{C}^2$  to a product torus. The space  $\mathcal{L}(X)$  is equipped with the smooth topology.

## 2. Introduction

A fundamental problem in symplectic topology is to understand the space of Lagrangian submanifolds, denoted by  $\mathcal{L}(X)$ , of a given manifold  $X$ , and in particular the action of the Hamiltonian group  $\text{Ham}(X)$  on  $\mathcal{L}(X)$ . We will describe some steps in this direction when the symplectic manifold is a domain in  $\mathbb{R}^4$ , including balls, integral ellipsoids, and polydisks. Our Lagrangian submanifolds are tori, and for simplicity we will restrict attention to those which are Hamiltonian isotopic to a product torus  $L(r, s)$  defined in (1). Recall that when  $X = \mathbb{R}^4$  the only known Lagrangian tori which do not fall into this category are Hamiltonian isotopic to scalings of the Chekanov torus, see [CS10].

The Lagrangian tori in a given domain  $X$  are described up to Hamiltonian diffeomorphism in  $\mathbb{R}^4$  by the (Hamiltonian) shape invariant

$$\text{Sh}_H(X) := \{(r, s) \in \mathbb{R}_{>0}^2 \mid L(r, s) \hookrightarrow X\}. \tag{2}$$

The study of the shape invariant was initiated by Eliashberg in [Eli91]. Note that  $\text{Sh}_H(X)$  contains strictly more information than the possible area classes of embedded Lagrangian tori (which we simply called the shape invariant in [HZ21]). Indeed the product tori  $L(1, 2)$  and  $L(2, 3)$  have integral Maslov 2 bases with the same area classes, but as stated in Theorem 2.1,  $L(1, 2) \hookrightarrow B(3 + \epsilon)$  for any arbitrarily small  $\epsilon > 0$  while there is no such embedding from  $L(2, 3)$ .

It is often convenient to work with the reduced Hamiltonian shape invariant denoted by  $\text{Sh}_H^+(X) := \text{Sh}_H(X) \cap \{r \leq s\}$ . As examples, the Hamiltonian shape invariants of balls  $B^4(R)$  and polydisks  $P(c, d)$  were worked out by the first author and Opshtein in [HO20], and the current authors computed the Hamiltonian shape invariant of integral ellipsoids in Theorem 1.8 in [HZ21].

**THEOREM 2.1** [HO20, HZ21]. *We have the following computations of the reduced Hamiltonian shape invariants.*

(i) When  $X = B^4(R)$ ,

$$\text{Sh}_H^+(B^4(R)) = \left\{ (r, s) \in \mathbb{R}_{>0}^2 \mid r + s < R \text{ or } r < \frac{R}{3} \right\} \cap \{r \leq s\}.$$

(ii) When  $X = E(a, b)$  with  $b/a \in \mathbb{N}_{\geq 2}$ ,

$$\text{Sh}_H^+(E(a, b)) = \left\{ (r, s) \in \mathbb{R}_{>0}^2 \mid \frac{r}{a} + \frac{s}{b} < 1 \text{ or } r < \frac{a}{2} \right\} \cap \{r \leq s\}.$$

(iii) When  $X = P(c, d)$  with  $0 < c \leq d$ ,

$$\text{Sh}_H^+(P(c, d)) = \left\{ (r, s) \in \mathbb{R}_{>0}^2 \mid \begin{array}{l} r < c \\ s < d \end{array} \text{ or } r < \frac{c}{2} \right\} \cap \{r \leq s\}.$$

*Remark 2.2.* (i) Note that the subsets  $\text{Sh}_H^+$  of the basic toric domains in Theorem 2.1 are all formed, modulo the intersection with  $\{r \leq s\}$ , by the moment image  $\mu(X)$  plus a vertical long strip.

(ii) The proof of statement (ii) in Theorem 2.1 utilized some results from Siegel [Sie22]; the results in the current paper are independent of Theorem 2.1.

**2.1 Hamiltonian knottedness**

There exists a Hamiltonian diffeomorphism of  $\mathbb{R}^4$  mapping  $L(r, s)$  onto  $L(r', s')$  if and only if  $\{r, s\} = \{r', s'\}$ , see [Che96]. Hence, there is a well-defined projection map

$$\mathcal{P} : \mathcal{L}(X) \rightarrow \text{Sh}_H^+(X) \tag{3}$$

mapping a Lagrangian torus in  $L \in \mathcal{L}(X)$  to the unique  $(r, s)$  such that  $r \leq s$  and  $L$  is Hamiltonian isotopic to  $L(r, s)$ .

This map is continuous. Indeed, by Weinstein’s neighborhood theorem, a sequence of Lagrangians  $L_n \rightarrow L$  in  $\mathcal{L}(X)$  can be thought of as sections of  $T^*L$  or, up to a Hamiltonian diffeomorphism, as sections of the normal bundle  $T^*L(r, s)$  of a product torus, where  $\mathcal{P}(L) = (r, s)$ . Such sections are Hamiltonian isotopic to constant sections, which correspond to  $L(r_n, s_n)$ , for  $(r_n, s_n)$  converging to  $(r, s)$ .

The Hamiltonian diffeomorphism group  $\text{Ham}(X)$  acts on  $\mathcal{L}(X)$  and preserves the fibers of  $\mathcal{P}$ . Paths in a fiber correspond to Lagrangian isotopies with a fixed area class  $(r, s) \in \text{Sh}_H^+(X)$ , and these are realized by a Hamiltonian isotopy in  $X$ , see Theorem 0.4.2 in [Cha83]. Hence, path connected components of the fibers are precisely the orbits of  $\text{Ham}(X)$ , and if a fiber over a point  $(r, s)$  happens to be disconnected, then we have embeddings  $L(r, s) \hookrightarrow X$  which are not Hamiltonian isotopic in  $X$ . This motivates the following definition.

**DEFINITION 2.3.** Suppose the product Lagrangian torus  $L(r, s)$  embeds into  $X$  by inclusion, i.e.  $(r, s) \in \mu(X)$ . Then we call an embedded Lagrangian torus in  $X$  *unknotted* if it is in the same component as  $L(r, s)$ , and *knotted* if it lies in another component.

More explicitly, if  $L(r, s) \subset X$ , then an embedded Lagrangian torus  $L \in \mathcal{P}^{-1}((r, s))$  is unknotted if there exists a Hamiltonian isotopy in  $X$ , denoted by  $\{\Phi_t\}_{t \in [0,1]}$ , such that  $\Phi_0 = \mathbb{1}_X$  and  $\Phi_1(L) = L(r, s)$ . Note that, for  $(r, s)$  with  $r \neq s$ , even though all Lagrangian tori in the fiber  $\mathcal{P}^{-1}((r, s))$  are conjectured to be Hamiltonian isotopic in  $\mathbb{R}^4$ , they are not necessarily Hamiltonian isotopic in  $X$ . In other words, the action of  $\text{Ham}(X)$  on a fiber of  $\mathcal{P}$  may not be transitive.

*Remark 2.4.* The (un)knottedness defined in Definition 2.3 is identical to that for symplectic embeddings discussed in [McD91, McD09, CG19, GU19].

Our first result says that for some basic domains many fibers of the projection  $\mathcal{P}$  are indeed disconnected, so knotted Lagrangian tori are quite common.

**THEOREM 2.5.** *Let  $X = B^4(R)$ . Then for any area classes*

$$(r, s) \in \Delta(R, R) \cap \{(r, s) \in \text{Sh}_H^+(X) \mid 3r \leq R \text{ and } 2r + s > R\}, \tag{4}$$

*there exist knotted Lagrangian tori in the fiber  $\mathcal{P}^{-1}((r, s))$ .*

**THEOREM 2.6.** *Let  $X = E(a, b)$  with  $k := b/a \in \mathbb{N}_{\geq 2}$ . Then for any area classes*

$$(r, s) \in \Delta(a, b) \cap \{(r, s) \in \text{Sh}_H^+(X) \mid 2r \leq a \text{ and } (k + 1)r + s > b\}, \tag{5}$$

*there exist knotted Lagrangian tori in the fiber  $\mathcal{P}^{-1}((r, s))$ .*

**THEOREM 2.7.** *Let  $X = P(c, d)$ . Then for any area classes*

$$(r, s) \in \square(c, d) \cap \{(r, s) \in \text{Sh}_H^+(X) \mid 2r \leq c \text{ and } r + s > d\}, \tag{6}$$

*there exist knotted Lagrangian tori in the fiber  $\mathcal{P}^{-1}((r, s))$ .*

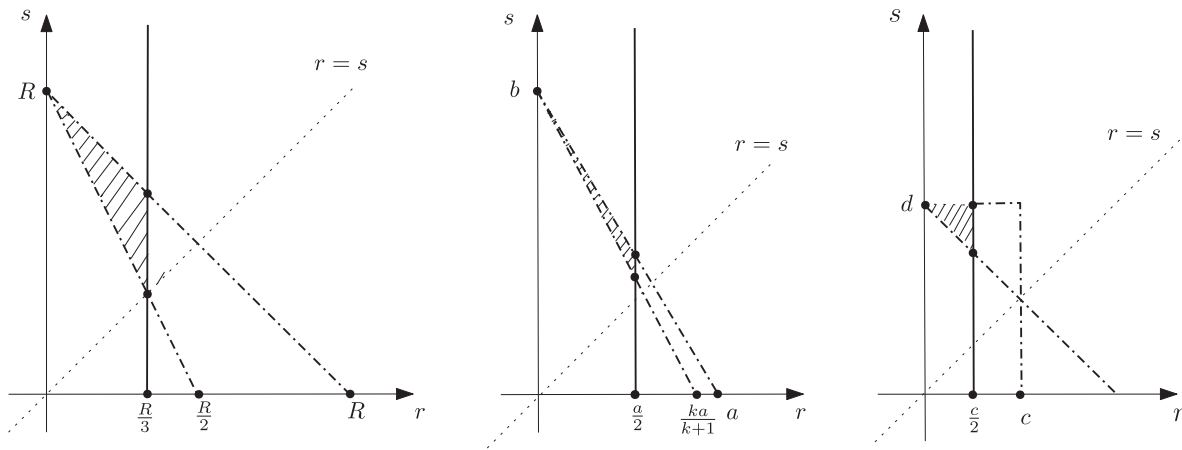


FIGURE 1. Regions that admit knotted Lagrangian tori.

The shaded parts in Figure 1 illustrate those regions claimed in Theorems 2.5, 2.6, and 2.7, respectively, where there exist knotted Lagrangian tori. Their proofs will be given in § 5.3. In fact, these results quickly follow from the path lifting properties that are systematically studied in § 2.2.

We remark that knotted Lagrangian tori in the ball were originally constructed by Vianna [Via14]. The exotic Lagrangian torus constructed by Chekanov [Che96] is not considered here as it is not Hamiltonian isotopic to a product torus in  $\mathbb{C}^2$ .

Detecting Hamiltonian knotted Lagrangian tori has connections to symplectic embeddings, and sometimes we can detect more knotted Lagrangian tori in both  $E(a, b)$  and  $B^4(R)$  by using our path lifting results together with the existence of symplectic embeddings. We will discuss this in detail in § 2.3.

It is also interesting to study Lagrangian knottedness in closed symplectic manifolds. In our case, we show that the knotted Lagrangians in the ball described by Theorem 2.5 are still not Hamiltonian isotopic to the corresponding product in the compactification  $\mathbb{C}P^2$ . Here we view  $\mathbb{C}P^2$  as the union of the ball  $B(R)$  and the line at infinity, which is a symplectic sphere of area  $R$ . Thus, we can strengthen Theorem 2.5 as follows.

**THEOREM 2.8.** *For any point  $(r, s)$  in (4), there exists a Lagrangian torus  $L \subset B^4(R) \subset \mathbb{C}P^2$  such that:*

- (i)  $\mathcal{P}(L) = (r, s)$ ;
- (ii)  $L$  is not Hamiltonian isotopic to  $L(r, s)$  in  $\mathbb{C}P^2$ .

We remark that Theorem 2.8 does not exclude the possibility that  $L$  is isotopic to another product torus in  $\mathbb{C}P^2$ . Indeed, according to [STV18], § 7, it is plausible to conjecture that almost all Lagrangian tori in  $\mathbb{C}P^2$  are Hamiltonian isotopic to product tori.

**2.2 Path lifting**

The main results in § 2.1 are consequences of a novel analysis of the path lifting problem of the projection  $\mathcal{P}$ . To start, let us give the following key definition.

**DEFINITION 2.9.** A smooth path  $\gamma : [0, T] \rightarrow \text{Sh}_H^+(X)$  where  $\gamma(0) = (r_0, s_0)$  lifts to  $\mathcal{L}(X)$  if there exists a smooth family of embedded Lagrangian tori in  $X$ , denoted by  $\{L_t\}_{t \in [0, T]}$ , with  $\mathcal{P}(L_t) = \gamma(t)$  and  $L_0 = L(r_0, s_0)$ .

In other words, unless stated otherwise, we will always assume our lifts start from an inclusion, and so a necessary condition for a lift is that  $\gamma(0) \in \mu(X)$ . In addition, denote by  $\mu(X)^+ := \mu(X) \cap \{r \leq s\}$ .

*Example 2.10.* For any smooth path  $\gamma : [0, T] \rightarrow \mu(X)^+ \subset \text{Sh}_H^+(X)$ , it lifts to  $\mathcal{L}(X)$  since one can consider the family of product Lagrangian tori  $\{L(r_t, s_t)\}_{t \in [0, T]}$  with area classes smoothly changing along  $\gamma$ .

We call any path in Example 2.10 a Type-I path, and any other path in  $\text{Sh}_H^+(X)$  starting in  $\mu(X)^+$  a Type-II path. We will elaborate on the subtlety of this path lifting from the following three perspectives, with more details given in § 7.

- (1) (*Concatenation*) One can build up a path that lifts to  $\mathcal{L}(X)$  via a series of concatenations of multiple sub-paths in either Type-I or Type-II, see Corollary 5.6 and also the left picture in Figure 18.
- (2) (*Non-uniqueness*) The path liftings are not unique. There exist paths  $\gamma$  having two lifts  $\{L_t\}_{t \in [0, T]}$  and  $\{L'_t\}_{t \in [0, T]}$  such that  $L_T$  and  $L'_T$  lie in different components of the fiber over  $\gamma(T)$ , see Remark 5.7.
- (3) (*Orientation*) Again, the right picture in Figure 18 shows that there exist paths with  $\gamma(0), \gamma(T) \in \mu(X)$  such that  $\gamma$  lifts but its reverse  $\bar{\gamma} := \{\gamma(T - t)\}_{t \in [0, T]}$  does not lift.

Next, we give both necessary and sufficient conditions (unfortunately not quite the same) for paths in the reduced (Hamiltonian) shape invariant of balls, integral ellipsoids, and polydisks to lift. For simplicity, we will state the results only for certain Type-II paths. More general paths can be considered via concatenations mentioned previously (see Corollary 5.6).

**THEOREM 2.11** (Path lifting for  $B^4(R)$ ). *Let  $\gamma = \{\gamma(t)\}_{t \in [0, T]}$  be a path in  $\text{Sh}_H^+(B^4(R))$  with  $\gamma(0) \in \mu(B^4(R))^+$  but  $\gamma(T) \notin \mu(B^4(R))^+$ . Denote  $\gamma(t) = (r_t, s_t)$ , then we have the following conclusions.*

- (I) *If  $r_t/s_t$  is non-increasing and  $2r_t + s_t \geq R$  for all  $t \in [0, T]$ , then  $\gamma$  does not lift to  $\mathcal{L}(B^4(R))$ .*
- (II) *The path  $\gamma$  does lift to  $\mathcal{L}(B^4(R))$  if there exists a  $t_*$  with  $0 \leq t_* \leq T$  satisfying:*
  - (i)  $\gamma|_{[0, t_*]} \in \mu(B^4(R))^+$ ;
  - (ii)  $2r_{t_*} + s_{t_*} < R$ ;
  - (iii)  $0 < r_t < R/3$  for any  $t \in [t_*, T]$ .

**THEOREM 2.12** (Path lifting for integral  $E(a, b)$ ). *Let  $\gamma = \{\gamma(t)\}_{t \in [0, T]}$  be a path in  $\text{Sh}_H^+(E(a, b))$  with  $k := b/a \in \mathbb{N}_{\geq 2}$ ,  $\gamma(0) \in \mu(E(a, b))^+$  but  $\gamma(T) \notin \mu(E(a, b))^+$ . Denote  $\gamma(t) = (r_t, s_t)$ , then we have the following conclusions.*

- (I) *If  $r_t/s_t$  is non-increasing and  $(k + 1)r_t + s_t \geq b$  for all  $t \in [0, T]$ , then  $\gamma$  does not lift to  $\mathcal{L}(E(a, b))$ .*
- (II) *The path  $\gamma$  does lift to  $\mathcal{L}(E(a, b))$  if there exists a  $t_*$  with  $0 \leq t_* \leq T$  satisfying:*
  - (i)  $\gamma|_{[0, t_*]} \in \mu(E(a, b))^+$ ;
  - (ii) *either one of the following conditions holds,*
    - (1)  $(k - 1)r_{t_*} \leq s_{t_*}$  and  $(k + 1)r_{t_*} + s_{t_*} < b$ , or
    - (2)  $(k - 1)r_{t_*} > s_{t_*}$  and  $0 < r_{t_*} < a/2$ ;
  - (iii)  $0 < r_t < a/2$  for all  $t \in [t_*, T]$ .

**THEOREM 2.13** (Path lifting for  $P(c, d)$ ). *Let  $\gamma = \{\gamma(t)\}_{t \in [0, T]}$  be a path in  $\text{Sh}_H^+(P(c, d))$  with  $\gamma(0) \in \mu(P(c, d))^+$  but  $\gamma(T) \notin \mu(P(c, d))^+$ . Denote  $\gamma(t) = (r_t, s_t)$ , then we have the following conclusions.*

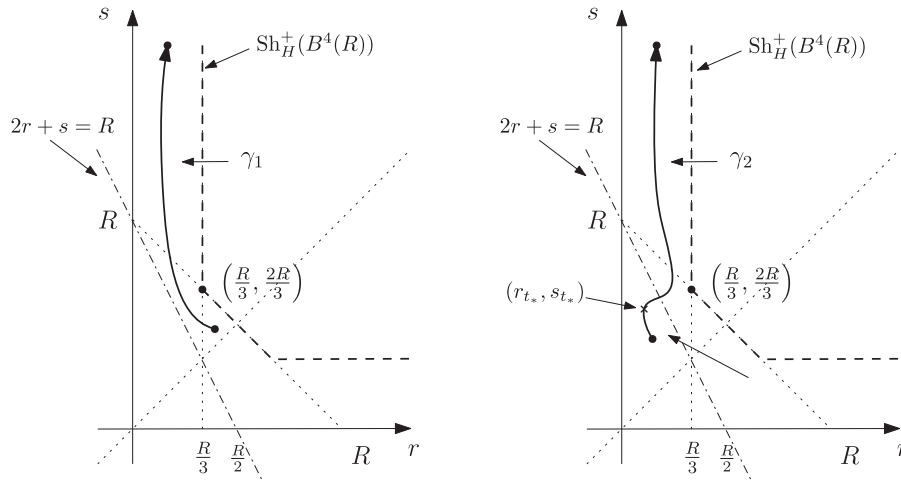


FIGURE 2. Path  $\gamma_1$  does not lift to  $\mathcal{L}(B^4(R))$  but  $\gamma_2$  does lift.

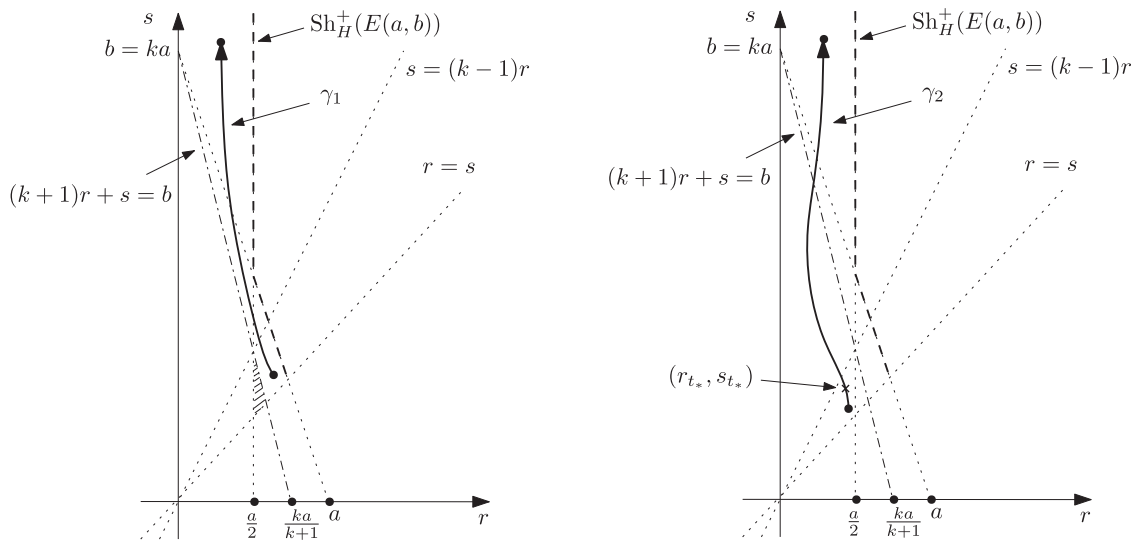


FIGURE 3. Path  $\gamma_1$  does not lift to  $\mathcal{L}(E(a,b))$  but  $\gamma_2$  does lift.

- (I) If  $r_t/s_t$  is non-increasing and  $r_t + s_t \geq d$  for all  $t \in [0, T]$ , then  $\gamma$  does not lift to  $\mathcal{L}(P(c, d))$ .
- (II) The path  $\gamma$  does lift to  $\mathcal{L}(P(c, d))$  if there exists a  $t_*$  with  $0 \leq t_* \leq T$  satisfying:
  - (i)  $\gamma|_{[0, t_*]} \in \mu(P(c, d))^+$ ;
  - (ii)  $r_{t_*} + s_{t_*} < d$ ;
  - (iii)  $0 < r_t < c/2$  for any  $t \in [t_*, T]$ .

*Example 2.14.* (1) The left picture in Figure 2 shows a path  $\gamma_1$  that does not lift to  $\mathcal{L}(B^4(R))$ , while the right-hand side shows a path  $\gamma_2$  that does lift. This is implied by Theorem 2.11.

(2) The left picture in Figure 3 shows a path  $\gamma_1$  that does not lift to  $\mathcal{L}(E(a, b))$ , while the right-hand side shows a path  $\gamma_2$  that does lift. This is implied by Theorem 2.12. In particular, for path  $\gamma_2$ , condition (II-ii-2) of Theorem 2.12 applies.

(3) The left picture in Figure 4 shows a path  $\gamma_1$  that does not lift to  $\mathcal{L}(P(c, d))$ , while the right-hand side shows a path  $\gamma_2$  that does lift. This is implied by Theorem 2.13.

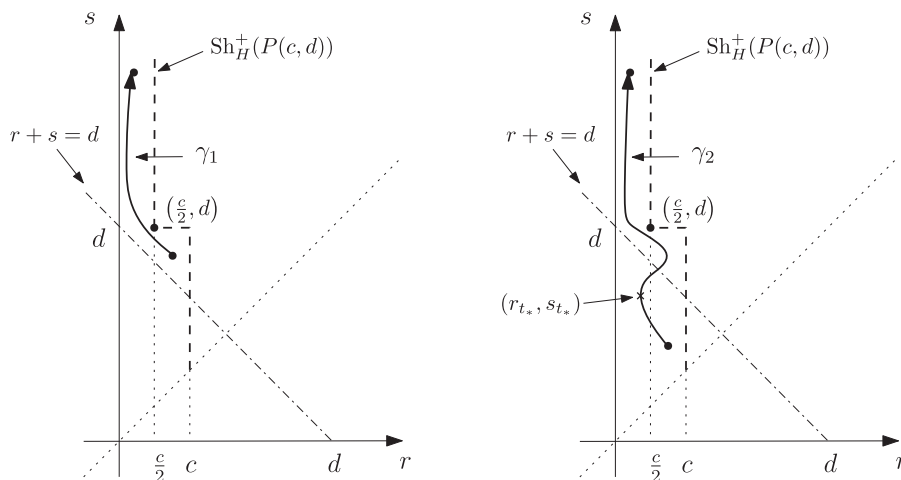


FIGURE 4. Path  $\gamma_1$  does not lift to  $\mathcal{L}(P(c, d))$  but  $\gamma_2$  does lift.

*Remark 2.15.* In Figure 3, suppose we deform  $\gamma_1$  such that the starting point lies in the shaded region, the endpoint is unchanged, and the new  $\gamma_1$  intersects  $\{(k + 1)r + s < b\}$  only in the shaded region. Then Theorem 2.12 is not strong enough to determine whether this path lifts or not. Indeed, such a  $\gamma_1$  does not satisfy condition (I) in Theorem 2.12 since the new starting point lies below the line  $(k + 1)r + s = b$ . But the new  $\gamma_1$  does not satisfy condition (II) in Theorem 2.12 either, since there exist no  $(r_{t_*}, s_{t_*})$  on the new  $\gamma_1$  which lie in the region described by condition (II-ii) in Theorem 2.12.

The obstructions (I) in Theorems 2.11 and 2.12 can be viewed as a single result (where for the case  $B^4(R)$ , we set  $k = 1$ ) and it will be proved in § 4.2; obstruction (I) in Theorem 2.13 has a similar proof, given in § 4.3. Results (II) in Theorems 2.11, 2.12, and 2.13, which will be proved in § 5.2, are consequences of a general path lifting criterion that works for any toric domains in  $\mathbb{R}^4$ , see Corollary 5.6 in § 5.1.

### 2.3 Symplectic embeddings

If there exists a Hamiltonian diffeomorphism  $f : X \hookrightarrow Y$ , then we have  $\text{Sh}_H^+(X) \subset \text{Sh}_H^+(Y)$  (see Proposition 7.1 in [HZ21]). Given its natural scaling properties, we can therefore think of  $\text{Sh}_H^+(X)$  as a kind of set-valued symplectic capacity. For a possible relation between this set-valued symplectic capacity and classical  $\mathbb{R}_{\geq 0}$ -valued symplectic capacities, see § 1.2.1 in [HZ21]. Some resulting obstructions to symplectic embeddings were explored in Theorem 1.6 in [HZ21], however at least in the case when  $X$  and  $Y$  are ellipsoids the obstructions turn out to be fairly weak, and are all consequences of Gromov’s non-squeezing together with the volume constraint.

Now we analyze embedding obstructions coming from shapes from the path lifting perspective. Observe that if  $\gamma : [0, T] \rightarrow \text{Sh}_H^+(X)$  is a path with  $\gamma(0) \in \mu(X)^+ \cap \mu(Y)^+$ , then, given our symplectic embedding  $\phi : X \hookrightarrow Y$ , if  $\gamma$  lifts as  $\{L_t\}_{t \in [0, T]}$  to  $\mathcal{L}(X)$ , then  $\{\phi(L_t)\}_{t \in [0, T]}$  gives a lift to  $\mathcal{L}(Y)$ , although this lift to  $\mathcal{L}(Y)$  may not satisfy our usual initial condition, that is,  $\phi(L_0) = L(\mathcal{P}(\gamma(0)))$ , a product torus in  $Y$ . However, applying a Hamiltonian diffeomorphism of  $Y$ , the initial condition can be satisfied if  $\phi(L_0)$  is unknotted in  $Y$ . Hence, we produce either examples of knotted Lagrangian tori in  $Y$  or potentially stronger embedding obstructions from  $X$  to  $Y$ . We have several consequences in these two directions.

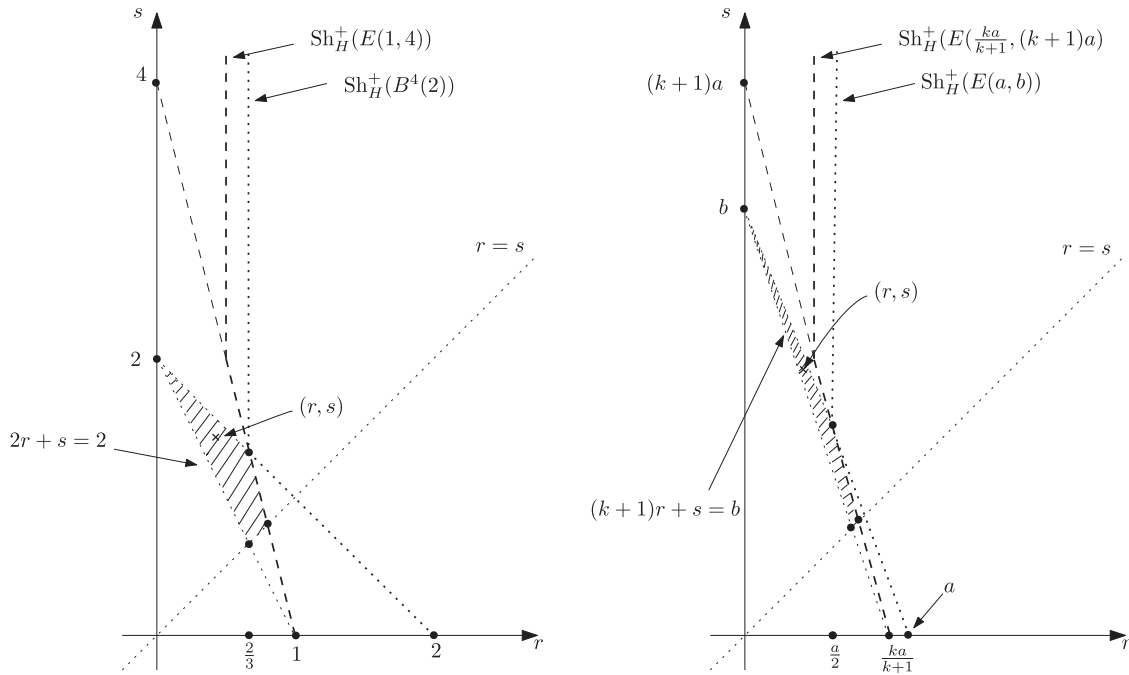


FIGURE 5. Knotted Lagrangian tori in  $B(2)$  and  $E(a, b)$  lie in the shaded regions.

2.3.1 *Detecting knotted Lagrangian tori.* The following result provides another approach (cf. Theorems 2.5, 2.6, and 2.7) to detect knotted Lagrangian tori. It will be proved in §8.1.

**THEOREM 2.16.** *We can detect knotted Lagrangian tori in the following three cases.*

- (1) *Suppose there exists a symplectic embedding  $\phi : E(1, x) \hookrightarrow B^4(R)$  for  $1 < R < x$ . If  $(r, s) \in \mu(E(1, x))^+ \cap \mu(B^4(R))^+$  with  $2r + s > R$ , then the embedded Lagrangian torus  $\phi(L(r, s))$  is knotted in the fiber  $\mathcal{P}^{-1}((r, s))$  of  $B^4(R)$ .*
- (2) *Suppose there exists a symplectic embedding  $\phi : E(1, x) \hookrightarrow E(a, b)$  for  $1 < a < b = ka < x$  with  $k \in \mathbb{N}_{\geq 2}$ . If  $(r, s) \in \mu(E(1, x))^+ \cap \mu(E(a, b))^+$  with  $(k + 1)r + s > b$ , then the embedded Lagrangian torus  $\phi(L(r, s))$  is knotted in the fiber  $\mathcal{P}^{-1}((r, s))$  of  $E(a, b)$ .*
- (3) *Suppose there exists a symplectic embedding  $\phi : E(1, x) \hookrightarrow P(c, d)$  for  $1 < c < d < x$ . If  $(r, s) \in \mu(E(1, x))^+ \cap \mu(P(c, d))^+$  with  $r + s > d$ , then the embedded Lagrangian torus  $\phi(L(r, s))$  is knotted in the fiber  $\mathcal{P}^{-1}((r, s))$  of  $P(c, d)$ .*

We emphasize that the knotted Lagrangian tori produced by Theorems 2.5, 2.6, and 2.7 are actually subsets of those which follow from Theorem 2.16 together with symplectic embedding results. In what follows, we provide examples to support this. One can quickly see the difference by comparing Figure 1 with Figures 5 and 6. In particular, we produce knotted Lagrangian tori with area class  $(r, s)$  such that  $r > R/3$ ,  $r > a/2$ , and  $r > c/2$ , respectively, in the examples below. To obtain this enhancement we require information about symplectic embeddings, while the knotted Lagrangian tori in Theorems 2.5, 2.6, and 2.7 are detected directly via the path lifting properties.

*Remark 2.17.* We remark that since the  $\phi$  in Theorem 2.16 are defined on ellipsoids, the knotted embedded tori  $\phi(L(r, s))$  extend to embedded polydisks  $\phi(P(r, s))$ , which of course must also be knotted.

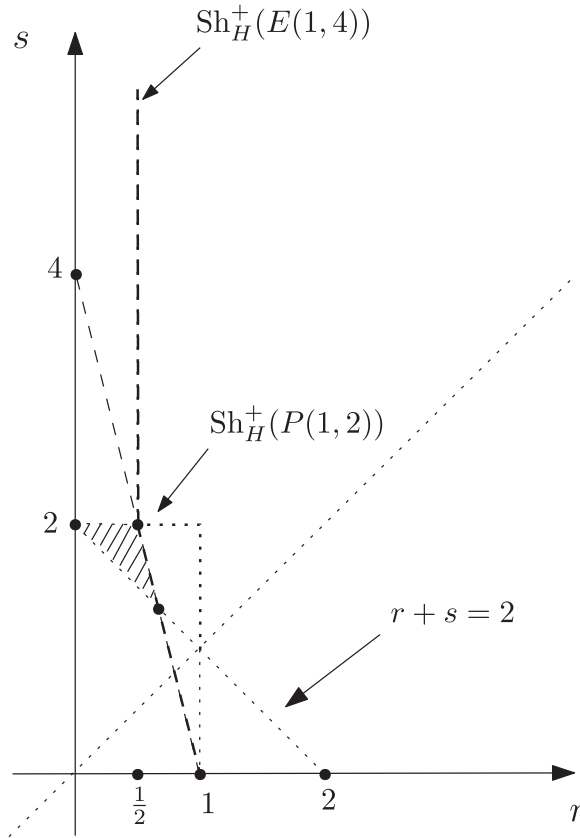


FIGURE 6. Knotted Lagrangian tori in  $P(1, 2)$  lie in the shaded region.

*Example 2.18.* (1) Let  $\phi : E(1, 4) \hookrightarrow B^4(2)$  be a symplectic embedding. We know such an embedding exists, see [Ops07, McDS12]. Any  $(r, s)$  in the shaded region in the left picture of Figure 5 satisfies criterion (1) of Theorem 2.16. Therefore,  $\phi(L(r, s))$  is knotted in the fiber  $\mathcal{P}^{-1}((r, s))$  of  $B^4(2)$ .

(2) Now let  $k \in \mathbb{N}_{\geq 2}$  and consider a symplectic embedding  $\phi : E(ka/(k + 1), (k + 1)a) \hookrightarrow E(a, b)$ . We verify in Appendix A that such embeddings do exist. Then, by Theorem 2.16(2) we see that  $\phi(L(r, s))$  is knotted in the fiber  $\mathcal{P}^{-1}((r, s))$  of  $E(a, b)$  provided  $(r, s) \in \mu(E(ka/(k + 1), (k + 1)a))^+ \cap \mu(E(a, b))^+$  with  $(k + 1)r + s > b$  or, in other words,

$$(r, s) \in \Delta(a, b) \cap \left\{ r \leq s \text{ and } (k + 1)r + \frac{ks}{k + 1} < b \text{ and } (k + 1)r + s > b \right\}. \tag{7}$$

Comparing with Theorem 2.6, this gives additional points in the region  $a/2 < r < b/(k + 1)$ .

Note that in the case of the ball  $B(R)$  we find knotted monotone Lagrangian tori projecting under  $\mathcal{P}$  to the interval  $\{(t, t) | R/3 < t < 2R/5\}$ . Vianna’s work [Via14] produces monotone tori projecting to the larger interval  $\{(t, t) | R/3 < t < R/2\}$ .

(3) Let  $\phi : E(1, 4) \hookrightarrow P(1, 2)$  be a symplectic embedding. We know such an embedding exists, see [CGFS17]. Any  $(r, s)$  in the shaded region in the left picture of Figure 6 satisfies criterion (3) of Theorem 2.16. Therefore,  $\phi(L(r, s))$  is knotted in the fiber  $\mathcal{P}^{-1}((r, s))$  of  $P(1, 2)$ .

Both the shaded regions in Figure 5 and the shaded region in Figure 6 contain strictly more points than those given by Theorems 2.5, 2.6, and 2.7. However, we need to confirm the existence

of a symplectic embedding when applying Theorem 2.16, which is sometimes non-trivial, see Proposition A.1 in Appendix A.

Here are a few immediate corollaries of Theorem 2.16 which can be compared with results on stabilized symplectic embeddings, see Theorem 1.1 in [McD18] or Theorems 1.1 and 1.3 in [CGHS22].

**COROLLARY 2.19.** *Denote by  $\overline{E(1, x)}$  the closure of the open ellipsoid  $E(1, x)$  in  $\mathbb{C}^2$ . We have the following conclusions.*

- (1) *If  $\overline{E(1, x)} \hookrightarrow B^4(R)$  and the image of  $L(x/(x + 1), x/(x + 1)) \subset \partial\overline{E(1, x)}$  is unknotted in  $B^4(R)$ , then  $R \geq 3x/(x + 1)$ .*
- (2) *If  $\overline{E(1, x)} \hookrightarrow E(a, b)$  with  $k := b/a \in \mathbb{N}_{\geq 2}$  and the image of  $L(x/(x + k - 1), (k - 1)x/(x + k - 1)) \subset \partial\overline{E(1, x)}$  is unknotted in  $E(a, b)$ , then  $a \geq 2x/(x + k - 1)$ .*
- (3) *If  $\overline{E(1, x)} \hookrightarrow P(c, d)$  with  $k := d/c \in \mathbb{R}_{>0}$  and the image of  $L(x/(x + 2k - 1), (2k - 1)x/(x + 2k - 1)) \subset \partial\overline{E(1, x)}$  is unknotted in  $P(c, d)$ , then  $c \geq 2x/(x + 2k - 1)$ .*

*Proof.* (1) The description of  $\text{Sh}_H^+(B^4(R))$  in Theorem 2.1 together with our embedding  $L(x/(x + 1), x/(x + 1)) \subset \overline{E(1, x)} \hookrightarrow B^4(R)$  implies that  $R > 2x/(x + 1)$ . Then

$$\left(\frac{x}{x + 1}, \frac{x}{x + 1}\right) \in \mu^+(\overline{E(1, x)}) \cap \mu^+(B^4(R))^+.$$

Hence, Theorem 2.16(1) implies that  $R \geq 2 \cdot x/(x + 1) + x/(x + 1) = 3x/(x + 1)$ .

(2) Without loss of generality, assume  $1 \leq a$  and  $x \geq b$ . As  $L(x/(x + k - 1), (k - 1)x/(x + k - 1)) \subset \overline{E(1, x)} \hookrightarrow E(a, b)$  we have  $(x/(x + k - 1), (k - 1)x/(x + k - 1)) \in \text{Sh}_H^+(E(a, b))$ . Therefore,

$$\left(\frac{x}{x + k - 1}, \frac{(k - 1)x}{x + k - 1}\right) \in \mu^+(\overline{E(1, x)}) \cap \mu^+(E(a, b))$$

since this point lies on the line  $s = (k - 1)r$  and any points in  $\text{Sh}_H^+(E(a, b) \setminus \mu^+(E(a, b)))$  have  $s > kr$  (cf. Figure 3). Hence, Theorem 2.16(2) implies that  $b \geq (k + 1) \cdot x/(x + k - 1) + (k - 1)x/(x + k - 1) = 2kx/(x + k - 1)$ . Dividing by  $k$  on both sides, we obtain the desired conclusion.

(3) Without loss of generality, assume  $1 \leq c \leq d \leq x$ . Now  $L(x/(x + 2k - 1), (2k - 1)x/(x + 2k - 1)) \subset \overline{E(1, x)} \hookrightarrow P(c, d)$  implies that  $(x/(x + 2k - 1), (2k - 1)x/(x + 2k - 1)) \in \text{Sh}_H^+(P(c, d))$ . Therefore,

$$\left(\frac{x}{x + 2k - 1}, \frac{(2k - 1)x}{x + 2k - 1}\right) \in \mu^+(\overline{E(1, x)}) \cap \mu^+(P(c, d))$$

since this point lies on the line  $s = (2k - 1)r$  and any points in  $\text{Sh}_H^+(P(a, b) \setminus \mu^+(P(a, b)))$  have  $s > 2kr$  (cf. Figure 4). Hence, Theorem 2.16(3) implies that  $d \geq x/(x + 2k - 1) + (2k - 1)x/(x + 2k - 1) = 2kx/(x + 2k - 1)$ . Dividing by  $k$  on both sides, we obtain the desired conclusion. □

*Remark 2.20.* A symplectic embedding  $\overline{E(1, x)} \hookrightarrow X$  is clearly a stronger condition than the existence of a family of Hamiltonian embeddings  $L(r, s) \hookrightarrow X$  for  $(r, s) \in \partial E(1, x)$ . However, since the bounds in Corollary 2.19 precisely match those in [CGHS22] we are naturally led to expect a close relation between Lagrangian isotopies and stabilized embeddings  $E(1, x) \times \mathbb{C} \hookrightarrow X \times \mathbb{C}$ . This will be explored elsewhere.

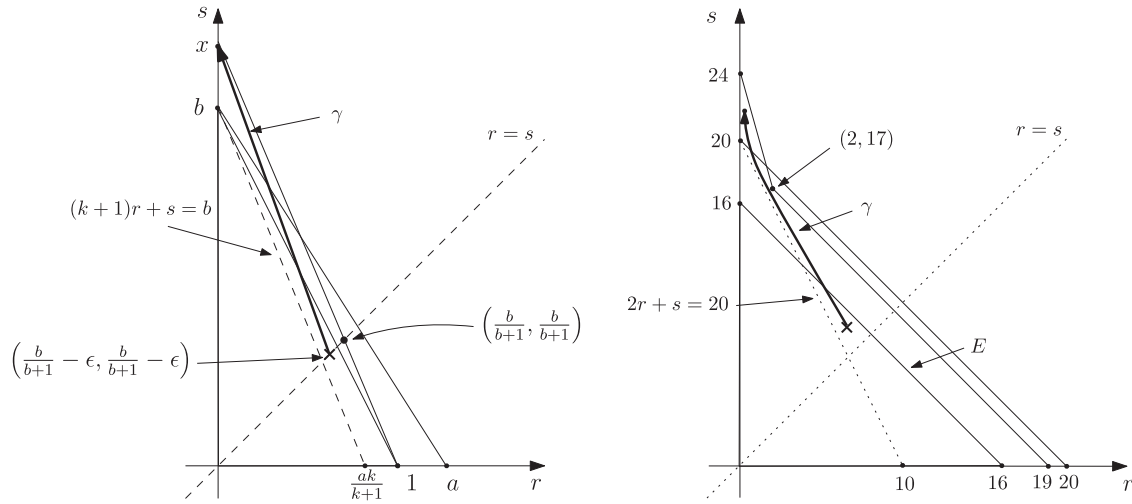


FIGURE 7. Embedding obstructions from path lifting.

2.3.2 *Embedding obstructions.* The obstructions to the symplectic embedding between toric domains are usually given by certain symplectic capacities, for instance, Ekeland–Hofer capacity [EH90], embedded contact homology (ECH) capacities [Hut11], Gutt–Hutchings capacities [GH18], etc. Almost all of them are constructed via dynamical information, e.g. closed Reeb orbits, on  $\partial X$  when it is viewed as a contact manifold with the contact structure induced by the standard primitive of the symplectic structure on  $\mathbb{R}^4$ . Until now, the cases that have been studied the most are toric concave domains and toric convex domains. By using the reduced (Hamiltonian) shape invariants, we are able to obtain embedding obstructions for a large family of toric star-shaped domains that are beyond the cases of toric concave or convex (see, e.g., the toric domain from the subset in  $\mathbb{R}_{\geq 0}^2$  bounded by the orange curve in Figure 19). Here is the result, which will be proved in §8.2.

THEOREM 2.21. *Let  $X \subset \mathbb{R}^4$  be a toric domain and  $E(a, b)$  an ellipsoid with  $k = b/a \in \mathbb{N}_{\geq 1}$ . Suppose  $X \not\hookrightarrow E(a, b)$ . If there exists an ellipsoid  $E$  satisfying the following conditions:*

- (i)  $E \subset X \cap E(a, b)$ , and  $E \not\hookrightarrow E(ak/(k + 1), b)$ ;
- (ii) *there exists an oriented path*

$$\gamma = \{(r_t, s_t) \in \mathbb{R}^2 \mid r_t \leq s_t\}_{t \in [0, T]} \subset \mu(X) \cap \mu\left(E\left(\frac{ak}{k + 1}, b\right)\right)^c \tag{8}$$

with  $(r_0, s_0) \in \mu(E)$ ,  $(r_T, s_T) \notin \mu(E(a, b))$ , and the ratio  $r_t/s_t$  non-increasing;

then there is no embedding  $X \hookrightarrow E(a, b)$ .

We illustrate the strength of Theorem 2.21 via the following corollaries. They provide obstructions to symplectic embeddings without computing any symplectic capacities.

COROLLARY 2.22. *Let  $E(a, b)$  be a symplectic ellipsoid with  $k := b/a \in \mathbb{N}_{\geq 2}$ . If there exists a symplectic embedding  $E(1, x) \hookrightarrow E(a, b)$  with  $1 < a < 1 + 1/k$ , then  $b \geq x$ .*

*Proof.* Suppose  $x > b$ , then see the left picture in Figure 7. Referring to Theorem 2.21 where  $X = E(1, x)$ , the desired ellipsoid  $E = X_{\Delta(1, b)}$  where  $\Delta(1, b)$  is the triangle with vertices  $(0, 0)$ ,  $(1, 0)$ , and  $(0, b)$ , and the desired path is the bold path (with arrow)  $\gamma$  in the picture. Therefore, Theorem 2.21 implies the contradiction. □

*Remark 2.23.* The result in Corollary 2.22 can also be derived from ECH capacities assuming a computational fact on the ECH capacities of 4-dimensional ellipsoids, namely Proposition 1.2 in [Hut11]. Explicitly, suppose  $b < x$ , let  $c_k^{\text{ECH}}$  denote the  $k$ th ECH capacity. One can verify that  $c_{k+1}^{\text{ECH}}(E(1, x)) > ak = b = c_{k+1}^{\text{ECH}}(E(a, b))$ .

**COROLLARY 2.24.** Consider toric domains  $B^4(20)$  and  $X_\Omega$  where the boundary  $\partial\Omega \cap \mathbb{R}_{>0}^2$  is piecewise linear with vertices  $(0, 24), (2, 17), (19, 0)$ , see the right picture in Figure 7. Then  $X_\Omega$  does not symplectically embed into  $B^4(20)$ .

*Proof.* By taking  $E = B^4(16)$  as the triangle  $\Delta(16, 16)$  with vertices  $(0, 0), (16, 0),$  and  $(0, 16)$  in the picture and  $\gamma$  as the bold path (with arrow) in the picture, Theorem 2.21 implies the desired conclusion. □

*Remark 2.25.* This embedding obstruction can also be derived from Gutt–Hutchings capacities denoted by  $c_k^{\text{GH}}$  and constructed in [GH18]. Explicitly, consider the second Gutt–Hutchings capacity. Since  $X_\Omega$  is a toric concave domain, by Theorem 1.14 in [GH18], one can verify that  $c_2^{\text{GH}}(X_\Omega) = 21 > 20 = c_2^{\text{GH}}(B^4(20))$ .

Finally, we include an example which seems beyond the reach of existing capacities: it is toric but not star-shaped, convex, nor concave.

**COROLLARY 2.26.** Fix  $S > 2R/3$  and  $R - S < u < S/2$ , and define

$$X_{S,u} = \overline{B^4(S)} \cup \bigcup_{S-u \leq v \leq R-u} L(u, v).$$

Then there is no symplectic embedding  $X_{S,u} \hookrightarrow B^4(R)$ .

*Proof.* Denote by

$$X_{S,u}(\delta) = B^4(S + \delta) \cup \bigcup_{S-u \leq v \leq R-u} L(u, v) \quad \text{for } \delta > 0.$$

Suppose there exists a symplectic embedding  $X_{S,u} \hookrightarrow B^4(R)$ . As the ball  $\overline{B^4(S)}$  in  $X_{S,u}$  is closed, any such embedding extends to a slightly larger ball. Therefore, we have a symplectic embedding  $X_{S,u}(\delta) \hookrightarrow B^4(R)$  for some sufficiently small  $\delta > 0$ . One can choose  $\delta$  such that  $S + \delta < R$ .

In order to apply Theorem 2.21, let us take  $E(a, b) = B^4(R)$  where  $a = b = R$  and  $k = 1$  as well as  $E = B^4(S + \delta)$ . Explicitly, (the closure of)  $E$  is the triangle  $\Delta(S + \delta, S + \delta)$  in Figure 8 with vertices  $(0, 0), (S + \delta, 0),$  and  $(0, S + \delta)$ . Note that  $X_{S,u}(\delta) \not\subset B^4(R)$  because the product Lagrangian torus  $L(u, R - u) \in X_{S,u}(\delta) \setminus B^4(R)$ . Moreover,  $E$  satisfies

$$E \subset X_{S,u}(\delta) \cap B^4(R) \quad \text{and} \quad E \not\subset E\left(\frac{R}{2}, R\right)$$

where the second relation comes from our hypothesis that  $S + \delta > S > 2R/3 > R/2$ . This verifies condition (i) in Theorem 2.21.

For condition (ii) in Theorem 2.21, let us take a path  $\gamma$  simply as

$$\gamma(t) = (u, (1 - t)(S - u) + t(R - u)) \quad \text{for } t \in [0, 1],$$

that is, the bold line segment (with arrow) in Figure 8. Obviously,  $\gamma \subset \mu(X_{S,u}(\delta))$ . Meanwhile, observe that  $\gamma(0) = (u, S - u)$  lies above the line  $s = R - 2r$  that describes the hypotenuse of the ellipsoid  $E(R/2, R)$  when  $S - u > R - 2u$  or  $u > R - S$ , and  $\gamma(0)$  lies in  $\{r \leq s\}$  provided  $u < S/2$ . (Parameters  $u$  satisfying both of these conditions exist when  $S > 2R/3$ .)

Hence, Theorem 2.21 is verified, and there are no symplectic embeddings  $X_{S,u}(\delta) \hookrightarrow B^4(R)$ . □

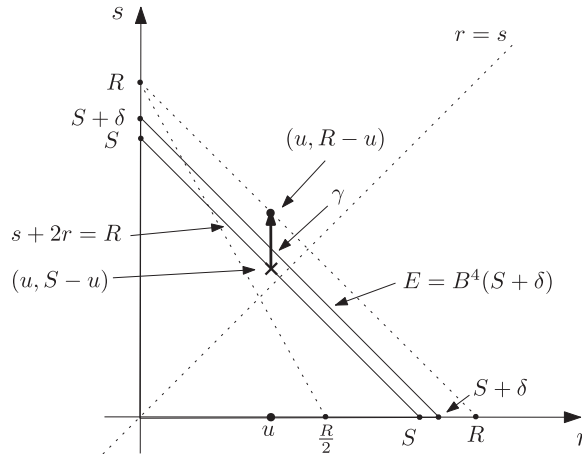


FIGURE 8. Embedding obstructions from path lifting.

*Remark 2.27.* Corollary 2.26 follows from the computation of the shape invariant in Theorem 2.1(i) (applied to  $L(u, R - u)$ ) only when  $u > R/3$ .

*Discussion.* For both Corollaries 2.22 and 2.24, one can deform the domain  $E(1, x)$  or  $X_\Omega$  to any star-shaped domains as long as we can find the desired ellipsoid  $E$  and a bold path (with arrow)  $\gamma$  as above, then still the embedding obstructions hold by Theorem 2.21. However, the classical symplectic capacities may not apply at all to the deformed domains. Moreover, the following two remarks are particularly interesting.

(1) In order to obtain the conclusion of Corollary 2.22, it is necessary to apply the obstruction from path lifting (instead of merely comparing the Hamiltonian shape invariants). Indeed, from  $\text{Sh}_H^+(E(1, x)) \subset \text{Sh}_H^+(E(a, b))$ , we only know that

$$\frac{a}{2} \geq \frac{1}{2} \quad \text{and} \quad \left(\frac{a}{2}, \frac{b}{2}\right) \text{ lies above the line } rx + s = x.$$

In other words,  $a \geq 1$  and  $b/2 \geq x - a/2 \cdot x$  (which is  $b \geq (2 - a)x$ ). Under the hypothesis that  $1 < a < 1 + 1/k$ , we have  $2 - a > 1 - 1/k$ , which implies that  $b \geq (1 - 1/k)x$ , and it is weaker than the conclusion of Corollary 2.22.

(2) The point  $(2, 17)$  on  $\partial\Omega$  in the hypothesis of Corollary 2.24 is crucial in the sense that it lies above the line  $2r + s = 20$ , so there is a sufficiently large space to produce the desired path  $\gamma \subset \mu(E(10, 20))^c$ . Curiously, the obstruction  $c_2^{\text{GH}}(X_\Omega) > c_2^{\text{GH}}(B^4(20))$  shows exactly this geometric property. It would be interesting to obtain an accurate relation between the path lifting obstruction and the capacities  $c_k^{\text{GH}}$ .

### 2.4 Related work

The papers [EGM18, STV18] study the star-shape of both open and closed symplectic manifolds. The star-shape is defined relative to a fixed Lagrangian torus  $L_0$  and in our language describes which *linear paths* have lifts starting at  $L_0$ . Here, rather than Hamiltonian isotopy class, lifts are defined in terms of flux, which makes sense on a general symplectic manifold. One of the main results in [EGM18] that relates to our work is a series of computations and estimations (via Poisson bracket invariant in [BEP12]) of the star-shape with different starting Lagrangians  $L_0$  in  $\mathbb{C}^n$ .

With more sophisticated algebraic machinery, e.g. Fukaya algebra, [STV18] enhances [EGM18] in various ways. A consequence of the main result in [STV18] is that for toric Fano varieties, the star-shape relative to the monotone Lagrangian fiber coincides with the moment polytope. In the case of  $B(R)$  this implies that linear paths starting from  $(R/3, R/3) \in \Delta(R, R)$  have lifts only if the path lies completely in the moment image  $\Delta(R, R)$ . We note that  $(R/3, R/3)$  lies precisely on the boundary of our ‘flexible region’  $\{2r + s < R\}$ , so the result matches Theorem 2.11. In this case our results cover more general paths, and we give constructions showing the constraints are often sharp. However, we emphasize that our obstructions rely on the non-triviality of certain moduli spaces of holomorphic curves, which are only established for simple domains.

The paper [STV18] also gives constructions of path lifts in  $\mathbb{C}P^2$  and other toric manifolds. While saying that two Lagrangians are not symplectomorphic in  $\mathbb{C}P^2$  is a stronger condition than Hamiltonian knottedness in the ball, if a path lifts in  $\mathbb{C}P^2$  the corresponding Lagrangian isotopy may intersect the line at infinity, and so these lifts do not imply lifting in the ball.

For detecting Hamiltonian knotted Lagrangian tori, Theorem 3.2 in Ono’s work [Ono15] detects the existence of knotted Lagrangian tori in  $P(c, c)$  with the area classes lying the following region

$$\square(c, c) \cap \{r \leq s \text{ and } r + s > c\}.$$

Note that this covers a larger region than that defined by (6) from Theorem 2.7 when  $c = d$ , but our result Theorem 2.7 applies to more general  $c$  and  $d$ .

### 3. Background and preliminary

#### 3.1 Shape invariant

Given an exact symplectic manifold  $(M^{2n}, \omega = d\lambda)$  with a fixed primitive  $\lambda$ , the shape invariant of this  $(M, \omega = d\lambda)$ , denoted by  $\text{Sh}(M, \lambda)$ , is defined as the collection of all possible area classes of embedded Lagrangian tori. More explicitly, for any Lagrangian embedding  $\phi : \mathbb{T}^n \hookrightarrow M^{2n}$ , the pullback  $\phi^*\lambda$  represents a cohomology class in  $H^1(\mathbb{T}^n; \mathbb{R})$ . By choosing an integral basis  $e := (e_1, \dots, e_n)$  of  $H_1(\mathbb{T}^n; \mathbb{Z})$ , the following evaluation

$$[\phi^*\lambda](e) = (\lambda(\phi_*(e_1)), \dots, \lambda(\phi_*(e_n))) \in \mathbb{R}^n \tag{9}$$

induces a map from Lagrangian embeddings to elements in  $\mathbb{R}^n$ . Of course, the set of values from (9) depends on  $\lambda$  and  $e$ , where a different choice of  $\lambda$  results in a uniform shift in  $\mathbb{R}^n$  and a different choice of  $e$  results in a transformation by an element in  $\text{GL}(n, \mathbb{Z})$ . In particular, the action by  $\text{GL}(n, \mathbb{Z})$  provides a certain symmetry of  $\text{Sh}(M, \lambda)$ . It is Sikorav’s work [Sik89] and Eliashberg’s work [Eli91] that first observed the application of the shape invariant to the study of the rigidity of symplectic or contact embeddings. For further development in this direction, see [Mül19, RZ21, HZ21].

In this paper, we consider a restrictive version of the shape invariant, called the *Hamiltonian shape invariant*, and our  $(M^{2n}, \omega = d\lambda) = (X, \omega_{\text{std}} = d\lambda_{\text{std}})$  for a toric domain  $X$  in  $(\mathbb{R}^4, \omega_{\text{std}})$ . It is defined in (2) as the collection of all possible area classes  $(r, s) \in \mathbb{R}_{>0}^2$  that admit  $L(r, s) \hookrightarrow X$ , and it is denoted by  $\text{Sh}_H(X)$ . Observe that in this set-up, there is no dependence of the primitive and we have a canonical choice of the basis  $e = (e_1, e_2)$ , where  $e_1$  is the standard circle in  $L(r, s)$ , lying in the first  $\mathbb{R}^2$ -factor of  $\mathbb{R}^4$ , bounding the disk with area  $r$  and  $e_2$  is the standard circle in  $L(r, s)$ , lying in the second  $\mathbb{R}^2$ -factor of  $\mathbb{R}^4$ , bounding the disk with area  $s$ . Then the only symmetry we have is via the reflection  $(r, s) \mapsto (s, r)$ , which induces a simplified version, the *reduced Hamiltonian shape invariant* denoted by  $\text{Sh}_H^+(X) := \text{Sh}_H(X) \cap \{r \leq s\}$ .

The explicit computations of  $\text{Sh}_H(X)$  as a subset in  $\mathbb{R}_{>0}^2$ , even for basic toric domains such as balls, ellipsoids, and polydisks, were carried out quite recently, see [HO20, HZ21]. Theorem 2.1 in the introduction summarizes the corresponding results. These results are consequences of a sophisticated analysis of holomorphic curves forming part of symplectic field theory (SFT).

A slightly different version of the shape invariant, which is formulated via the flux of a Lagrangian isotopy (in particular, applied on closed manifolds such as  $\mathbb{C}P^n$  and  $S^2 \times S^2$ ), has been studied in [EGM18, STV18]. These works point out the intriguing relations between the shape invariant and Poisson-bracket invariants in [BEP12] and the SYZ fibration in [SYZ96], respectively.

### 3.2 Symplectic field theory

Lagrangian embeddings  $\phi : L(s, t) \hookrightarrow X$  can be effectively studied via SFT. It is a modern machinery, originally formulated in the work [EGH00] and further developed in [BEH<sup>+</sup>03, Hof06, CM18], that can associate a variety of algebraic invariants to a symplectic cobordism. Our work, however, does not rely on this full algebraic machinery, which is indeed still under development. The proofs in the current paper require only compactness and deformation theorems for (somewhere injective) holomorphic curves, modulo some references to ECH and to earlier works of the authors. The input from these earlier works is used to establish existence of a holomorphic curve in Lemma 4.1 (which can be avoided using Remark 4.2) and then in the bubbling analysis of both §4.1.2 and the main proof in §4.2, where Lemma 3.7 of [HO20] is a key ingredient.

Topologically, our symplectic cobordism is the complement  $W := X \setminus U_g^*L$  where  $L = \phi(L(r, s))$  and  $U_g^*L$  is the unit codisk bundle of  $L$  with respect to some metric  $g$  on  $L$ ; our metrics will always be flat. With a preferred almost complex structure  $J$  on  $W$ , the central objects in SFT are  $J$ -holomorphic curves  $C : (S^2 \setminus \{p_1, \dots, p_m\}, j) \rightarrow (W, J)$ , where the asymptotic ends from punctures  $p_i$  correspond to Reeb orbits on  $\partial X$  (positive ends) and on  $S_g^*L := \partial U_g^*L$  (negative ends). In fact, the Reeb orbits on  $S_g^*L$  can readily be classified (see Proposition 3.1 in [HO20]). More concretely, we say a Reeb orbit on  $S_g^*L$  is of the type  $(-m, -n)$ , denoted by  $\gamma_{(m,n)}$ , if its projection to  $L$  lies in the homology class  $(-m, -n) \in H^1(\mathbb{T}^2, \mathbb{Z})$ . Note that for a  $J$ -holomorphic plane  $C : (S^2 \setminus \{p\}, j) \rightarrow (W, J)$  with only one asymptotic end on  $\gamma_{(-m,-n)}$ , by Stokes' theorem, its area is

$$\text{area}(C) = 0 - (r(-m) + s(-n)) = rm + sn (> 0).$$

A useful algebraic invariant of  $C$  is its Fredholm index. Denote by  $\{\gamma_i^+\}_{i=1}^{s_+}$  the collection of positive asymptotic orbits and  $\{\gamma_i^-\}_{i=1}^{s_-}$  the collection of negative asymptotic orbits. Without loss of generality, let us assume these Reeb orbits are either non-degenerate or Morse–Bott, that is, they may come in smooth families, and  $S_i^+$  and  $S_i^-$  are the leaf spaces of the associated Morse–Bott submanifolds. Fix a symplectic trivialization  $\tau$  of  $C^*TW$  along these Reeb orbits, and  $c_1^\tau(C^*TW)$  denotes the first Chern number with respect to this trivialization  $\tau$ . Then

$$\begin{aligned} \text{ind}(C) &= (s_+ + s_- - 2) + 2c_1^\tau(C^*TW) \\ &+ \left( \sum_{i=1}^{s_+} \text{CZ}^\tau(\gamma_i^+) + \frac{\dim S_i^+}{2} \right) - \left( \sum_{i=1}^{s_-} \text{CZ}^\tau(\gamma_i^-) - \frac{\dim S_i^+}{2} \right), \end{aligned} \tag{10}$$

where  $\text{CZ}^\tau$  is the Conley–Zehnder index with respect to  $\tau$ , which can be computed as the Robbin–Salamon index (see [RS93]). Note that  $\text{ind}(C)$  is independent of the choice of symplectic trivialization  $\tau$ . When specifying  $\gamma_i^- = \gamma_{(-m_i, n_i)}$  for  $i \in \{1, \dots, s_-\}$  and taking  $\tau$  as the complex trivialization of the contact planes induced by complexifying the trivialization of the 2-torus, the

index formula (10) can be computed by

$$\text{ind}(C) = (s_+ + s_- - 2) + \left( \sum_{i=1}^{s_+} \text{CZ}^\tau(\gamma_i^+) + \frac{\dim S_i^+}{2} \right) + 2 \sum_{i=1}^{s_-} (m_i + n_i). \tag{11}$$

For more detailed elaboration, see Example 4.1 in [HZ21]. Sometimes, the toric domain  $X$  can be compactified to be a closed symplectic manifold by adding certain curves at infinity. In this paper, we are particularly interested in the following two cases.

(i) Ball  $B^4(R)$ , where  $B^4(R)$  can be compactified to  $\mathbb{C}P^2(R)$  with the area of the line at infinity  $S_\infty$  being  $R$ . Then we study  $C$  without positive ends, but with a topological invariant given by its intersection number with  $S_\infty$ . We denote the intersection by  $d$ . Then the corresponding formula in (11) is

$$\text{ind}(C) = (s_- - 2) + 6d + 2 \sum_{i=1}^{s_-} (m_i + n_i). \tag{12}$$

(ii) Polydisks  $P(c, d)$ , where  $P(c, d)$  can be compactified to  $S^2(c) \times S^2(d)$  with two factors having areas  $c$  and  $d$ , by adding two curves  $\{\infty\} \times S^2(b)$  and  $S^2(a) \times \{\infty\}$ . Then we study  $C$  without positive ends, but with a topological invariant given by its intersection with these two curves at infinity. We denote by  $(d_1, d_2)$  the bidegree labeling the two intersection numbers. Then the corresponding formula in (11) is

$$\text{ind}(C) = (s_- - 2) + 4(d_1 + d_2) + 2 \sum_{i=1}^{s_-} (m_i + n_i). \tag{13}$$

A useful technique in SFT is neck-stretching, via a sequence of deformations of almost complex structures on the symplectic cobordism  $W$ . The standard SFT compactness theorem in [BEH<sup>+</sup>03] promises the existence of a limit curve  $C_{\text{lim}}$ , more precisely, a pseudo-holomorphic building consisting of curves in different levels matched in a possibly complicated way. However, the two invariants introduced above,  $\text{area}(C)$  and  $\text{ind}(C)$ , converge in the limit and behave in a rather controllable manner. To be precise, if  $C_{\text{lim}}$  is obtained by gluing different sub-buildings  $\{C_i\}_{i=1}^n$  along matching orbits  $\{\gamma_i\}_{i=1}^m$ , then

$$\text{area}(C_{\text{lim}}) = \text{area}(C_1) + \dots + \text{area}(C_n) \tag{14}$$

and

$$\text{ind}(C_{\text{lim}}) = \sum_{i=1}^n \text{ind}(C_i) - \sum_{i=1}^m \dim S_i, \tag{15}$$

where  $S_i$  is the leaf space of  $\gamma_i$  for  $i \in \{1, \dots, m\}$ . For more details, see Proposition 3.3 in [HO20]. In what follows, we will see that the combination of  $\text{area}(C)$  and  $\text{ind}(C)$  actually yield quite strong constraints on the possible configurations of  $C_{\text{lim}}$ . This will be essential to the study of embeddings  $L(r, s) \hookrightarrow X$ . These ideas were also used in both [HO20, HZ21] in the computations of the (Hamiltonian) shape invariant.

#### 4. Obstructions to path liftings

In this section, we will prove the obstruction to a path lifting, that is, obstruction (I) in Theorems 2.11, 2.12, and 2.13. We will deal with Theorems 2.11 and 2.12 together, although 2.11 could also be proved using a compactification as in our proof of Theorem 2.13. Before the main

proof we first establish the existence of a certain holomorphic cylinder, and then analyze possible degenerations of moduli spaces of genus 0 curves with Fredholm index at least equal to the number of negative ends.

### 4.1 Preparations

4.1.1 *Existence of a holomorphic cylinder.* The following lemma, Lemma 4.1, guarantees the existence of a holomorphic cylinder which will initiate our main proof.

Recall that  $L(r_0, s_0)$  is the product torus in  $\mathbb{C}^2$  with area classes  $r_0$  and  $s_0$ . We assume  $L(r_0, s_0) \subset E(a, b)$ , that is,  $kr_0 + s_0 < b$ . Recall that  $\gamma_{(m,n)}$  denotes the closed Reeb orbits of type  $(-m, -n)$  on the unit co-sphere bundle  $S_g^*L(r_0, s_0)$  with respect to a preferred flat metric  $g$  on  $L(r_0, s_0)$ . Since  $L(r_0, s_0) \subset E(a, b)$ , rescaling the metric  $g$ , we may assume this unit codisk bundle  $U_g^*L(r_0, s_0)$  sits inside  $E(a, b)$ . As discussed in § 3.2, the complement  $E(a, b) \setminus U_g^*L(r_0, s_0)$  is a symplectic cobordism and the deformed complex structure, denoted by  $J_0$ , gives a compatible almost complex structure with cylindrical ends. Denote by  $\gamma_b$  the long closed Reeb orbit on  $\partial E(a, b)$  with period  $b$ .

In order to guarantee non-degeneracy, when working with holomorphic curves asymptotic to ellipsoids we will always increase  $b$  slightly so that  $b/a \notin \mathbb{Q}$ . As the perturbation can be arbitrarily small this does not affect the statements of any of our results. Here, with our fixed trivialization  $\tau$  as in § 3.2, the longer orbit  $\gamma_b$  of  $E(a, b)$  has its Conley–Zehnder index given by  $CZ^\tau(\gamma_b) = 2 \lfloor b/a \rfloor + 3$ .

LEMMA 4.1. *There exists a  $J_0$ -holomorphic cylinder in the symplectic cobordism*

$$E(a, b) \setminus U_g^*L(r_0, s_0)$$

with a positive end on  $\gamma_b$ , the longer Reeb orbit of  $\partial E(a, b)$ , and with a negative end on a Reeb orbit  $\gamma_{k,1}$  on  $S_g^*L(r_0, s_0)$  (where recall  $k = b/a$ ).

*Outline of the proof of Lemma 4.1.* One proof of this is to analyze a neck-stretching argument in [HZ21] which produces a union of curves in the cobordism  $E(a, b) \setminus U_g^*L(r_0, s_0)$ , checking that one of the curves must be a cylinder as required. We also give a direct geometric construction in Remark 4.2 of a cylinder which is holomorphic for *some* almost complex structure (a result which is actually enough for our purposes).

*Proof of Lemma 4.1.* There exists a thin and long ellipsoid denoted by  $E(\epsilon, \epsilon S)$  which can be embedded inside the unit codisk bundle  $U_g^*L(r_0, s_0)$ . Here,  $\epsilon$  is sufficiently small and we require  $S > k + 1$ . Up to symplectomorphism, we have the following inclusions,

$$E(\epsilon, \epsilon S) \subset U_g^*L(r_0, s_0) \subset E(a, b).$$

Denote by  $\beta$  the short closed Reeb orbit of  $\partial E(\epsilon, \epsilon S)$  with period  $\epsilon$ . By an appropriate deformation of the almost complex structure, we can view  $E(a, b) \setminus E(\epsilon, \epsilon S)$  as a symplectic cobordism with respect to an almost complex structure (still) denoted by  $J_0$ . By Theorem 5.8 in [HZ21], there exists a  $J_0$ -holomorphic cylinder with positive end  $\gamma_b$  and negative end  $\beta^{k+1}$ .<sup>1</sup> Then by a neck-stretching along the boundary  $S_g^*L(r_0, s_0)$  as in [HZ21], Lemma 6.1, the limiting building  $C_{\text{lim}}$  contains  $(k + 2)$ -many curves in  $E(a, b) \setminus U_g^*L(r_0, s_0)$ , denoted by  $\{F_1, \dots, F_{k+2}\}$ . Lemma 6.1 in [HZ21] also implies that for each  $i \in \{1, \dots, k + 2\}$ , we have  $\text{ind}(F_i) = 1$ . Moreover, since we

<sup>1</sup> Strictly speaking, the statement of Theorem 5.8 in [HZ21] guarantees the existence of a curve with possibly more positive ends. However, it is easy to see that the gluing method in the proof of Theorem 5.8 in [HZ21], when applied to the cylinder provided by Lemma 5.6 in [HZ21] and a cylinder, labeled as  $C_{\text{HK}}$ , provided by [HK20], results in the cylinder desired here.

have only one positive end, the argument in the proof of the ‘only if’ part of Theorem 1.4 in [HZ21] implies that all but one of the  $F_i$  are planes and the remaining curve is a cylinder with positive end on  $\gamma_b$ . Without loss of generality, assume  $F_1$  is the cylinder. Moreover, suppose the negative end of  $F_i$  has type  $(-k_i, -l_i)$ . Since the negative ends bound a cycle in  $T^*L(r_0, s_0)$  we see

$$\sum_{i=1}^{k+2} k_i = \sum_{i=1}^{k+2} l_i = 0. \tag{16}$$

So far, we have implicitly assumed our  $J_0$  is generic in order to guarantee curves of non-negative index. However, we would like to work with a  $J_0$  such that the  $z_1$  and  $z_2$  axes are complex (and, hence, are finite energy planes, say  $P_1$  and  $P_2$ , asymptotic to  $\gamma_a$  and  $\gamma_b$ , respectively). As these axes are disjoint from  $L(r_0, s_0)$ , it is easy to check that they are not covered by any of our limiting curves, and so we may still assume regularity.

Since the axes are complex, positivity of intersection implies that for  $i \geq 2$  the  $F_i$  are asymptotic to a Reeb orbits representing classes with  $k_i \leq 0$  and  $l_i \leq 0$ . As the curves have index 1, the index formula implies that  $k_i + l_i = -1$ , so the only possibilities are  $(k_i, l_i) = (-1, 0)$  or  $(k_i, l_i) = (0, -1)$ . Identifying any matching asymptotic orbits and adding a disk inside  $E(\epsilon, \epsilon S)$ , our holomorphic building can be compactified to form a homology class in the ellipsoid with boundary  $\gamma_b$ . Since  $P_1$  represents a class with boundary  $\gamma_a$ , it has intersection number +1 with the compactified building. Then by positivity of intersection, we see that at most one  $F_i$  is asymptotic to an orbit in the class  $(0, -1)$ .

Suppose first that exactly one  $F_i$  for  $i \geq 2$  is asymptotic to an orbit of type  $(0, -1)$ . Then  $F_1$  is asymptotic to an orbit of type  $(k, 1)$  as required.

Alternatively, all  $F_i$  for  $i \geq 2$  are asymptotic to orbits of type  $(-1, 0)$  and  $F_1$  is asymptotic to an orbit of type  $(k + 1, 0)$ . In this case the limiting building has intersection number at least  $k + 1$  with  $P_2$ . However we can compute Siefring’s generalized intersection number (see (4-3) in [Sie11]) to be

$$P_2 * P_2 = k.$$

Indeed, trivializing the contact planes in  $E(a, b)$  along  $\partial P_2$  by using an identification  $\Phi$  with the  $z_1$  plane, in the notation from [Sie11] we have  $i^\Phi(P_2, P_2) = 0$  and  $\Omega^\Phi(P_2, P_2) = k$ .

As our limiting holomorphic building has a single unmatched positive end on  $\gamma_b$  and (after we compactify with the disk inside  $E(\epsilon, \epsilon S)$ ) is homotopic relative to its compactified positive boundary to  $P_2$ , Theorem 2.2 from [Sie11] implies that  $k$  is an upper bound for the intersections between the curves in our limiting building and  $P_2$ . This is a contradiction if the building contains  $k + 1$  planes asymptotic to  $(-1, 0)$ . □

*Remark 4.2.* For an alternative proof of Lemma 4.1, at least for a carefully chosen  $J_0$ , we observe it is, in fact, possible to write down such a holomorphic cylinder directly. To do this we fix a circle  $\Gamma = \{\theta_1 - k\theta_2 = 0\}$  in the torus  $\mathbb{T}^2$ , and identify all fibers of the moment map  $\mu$  with the same  $\mathbb{T}^2$ , suitably collapsed over the axes. In the moment image  $\mu(E(a, b))$  let  $\sigma$  be a curve which coincides with the line through  $(r_0, s_0)$  of slope  $1/k$  at one end, and the vertical line through  $(0, b)$  at the other. Then  $\sigma \times \Gamma$  is a cylinder in  $E(a, b)$ , which is symplectic provided  $\sigma$  never has slope  $-k$ . We can find such paths exactly because  $b > ka$ . Moreover, our cylinder coincides with the trivial cylinder over the Reeb orbits at each end, so we can find an almost complex structure  $J_0$  making the cylinder holomorphic.

4.1.2 *Degenerations of moduli spaces.* Here we analyze possible degenerations of a moduli space of genus 0 curves with Fredholm index bounded below by the number of negative ends.

In any degeneration we can isolate a particular limiting curve, and the main Lemma 4.4 shows that areas of curves in the new moduli space are bounded above by the areas of the original moduli space.

Given an isotopy of Lagrangian submanifolds  $\{L_t\}_{t \in [0,1]}$ , corresponding compatible almost complex structures  $J_t$  on the complement of  $L_t$ , and a sequence of  $J_{t_n}$ -holomorphic curves  $\{C_n\}_{n \in \mathbb{N}}$  with (negative) ends on the Lagrangian submanifolds  $\{L_{t_n}\}_{n \in \mathbb{N}}$ , the standard SFT-compactness implies that if  $t_n \rightarrow t_*$  and the  $C_n$  have bounded area, for example if they appear in the same moduli space, then the  $C_n$  converge to a  $J_{t_*}$ -holomorphic building  $C_{\text{lim}}$ . To be precise, the standard SFT-compactness applies to a sequence of  $J_n$ -holomorphic curves  $C_n$  in a fixed cobordism, however we can use Fukaya’s trick (see §2.1 in [STV18]) to transfer the moving boundary conditions on  $L_{t_n}$  to a sequence of almost complex structures on a fixed cobordism as required. Hence, we still obtain compactness as in [BEH<sup>+</sup>03]. A careful study of  $C_{\text{lim}}$  plays an important role in the proof of obstruction (I) in Theorems 2.11 and 2.12. In particular, the following technical lemma, Lemma 4.3, is useful to us.

Let  $C$  denote a curve with  $\text{ind}(C) = e$ , one positive end on  $\gamma_b$ , and  $e$ -many negative ends on the Lagrangian torus  $L_0$ . For instance, the cylinder provided by Lemma 4.1 satisfies this condition with  $L_o = L(r_0, s_0)$ , since by (11)

$$\text{ind}(C) = (2k + 3) - (2k + 2) = 1 = \# \text{ negative ends of } C.$$

Denote by  $\mathcal{M}_C(t)$  for  $t \in [0, 1]$  the moduli space corresponding to the curve  $C$  with boundary conditions on  $L_t$ . Suppose the universal moduli space of the  $\mathcal{M}_C(t)$  is not compact, that is, there exist a degeneration at  $t_* \in [0, 1]$  with a limiting building  $C_{\text{lim}} \notin \mathcal{M}_C(t_*)$ . The proof of Lemma 3.7 in [HO20, p. 552] shows there exists a curve of  $C_{\text{lim}}$  in  $E(a, b) \setminus U_g^* L_{t_*}$ , which we denote by  $C_0$ , having  $\text{ind}(C_0) \geq \# \text{ negative ends of } C_0$ . We denote by  $C_1, \dots, C_k$  the components (as connected sub-buildings of  $C_{\text{lim}}$  consisting of curves in  $E(a, b) \setminus U_g^* L_{t_*}$  and in the symplectization  $T^* L_{t_*} \setminus 0_{L_{t_*}}$ ) of the complement of  $C_0$  in  $C_{\text{lim}}$  such that each  $C_i$  matches with  $C_0$  at only one negative end of  $C_0$ . See Figure 9 for an example of  $C_{\text{lim}}$ . Suppose  $C_i$  for  $i \in \{1, \dots, k\}$  admits  $e_i$ -many negative ends, while the cardinality of the unmatched ends of  $C_0$  is denoted by  $e_0$  (hence, the total number of the negative ends of  $C_{\text{lim}}$  is  $\sum_{i=0}^k e_i$ ). Finally, as shown in Figure 9, suppose the negative ends of the curves in  $E(a, b) \setminus U_g^* L_{t_*}$  from the component  $C_i$  have type  $\{(-m_i^j, -n_i^j)\}_{j=1, \dots, l_i}$ . Then we have the following result.

LEMMA 4.3. *Suppose  $C_0$  contains the positive end  $\gamma_b$ . Then, with  $(-m_i^j, -n_i^j)$  defined as above, we have  $\sum_{i=1}^k \sum_{j=1}^{l_i} (m_i^j + n_i^j) \leq 0$ .*

*Outline of the proof of Lemma 4.3.* We will compare the indices of the various components  $C_i$  with the index of the limiting building using (15). Together with an analysis of matching ends we will derive the result.

*Proof of Lemma 4.3.* First, by the index matching formula (15), we have

$$e = \text{ind}(C_{\text{lim}}) = \left( \sum_{i=0}^k \text{ind}(C_i) \right) - k, \quad \text{which is} \quad \sum_{i=0}^k \text{ind}(C_i) = e + k. \tag{17}$$

Since  $e = \# \text{ negative ends of } C_{\text{lim}} = e_0 + \dots + e_k$ , by regrouping these terms, (17) is equivalent to the relation  $(\text{ind}(C_0) - (e_0 + k)) + \sum_{i=1}^k (\text{ind}(C_i) - e_i) = 0$ . Moreover, since  $e_0 + k$  equals the  $\#$  negative ends of  $C_0$ , by assumption,  $\text{ind}(C_0) \geq e_0 + k$ , so

$$\sum_{i=1}^k (\text{ind}(C_i) - e_i) \leq 0. \tag{18}$$

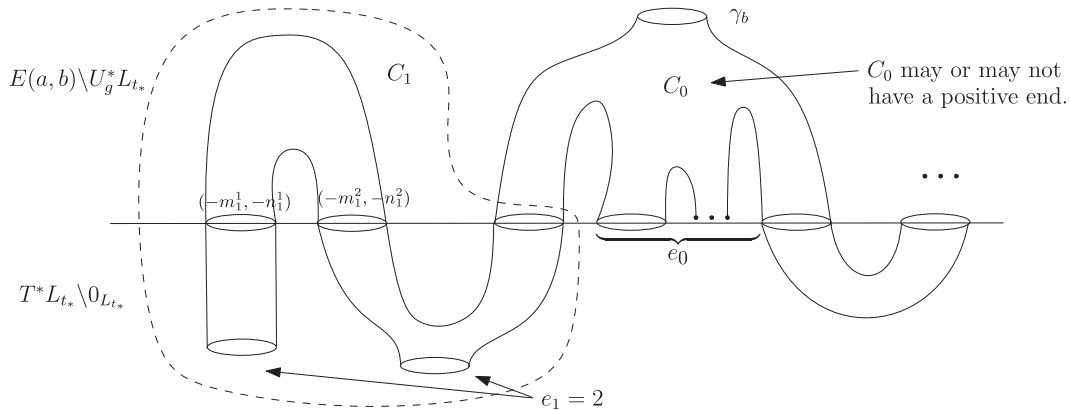


FIGURE 9. A limit curve in  $\mathcal{M}_C(t_*)$ .

Second, let us focus on a component  $C_i$  for  $i \in \{1, \dots, k\}$ . Since  $C_0$  already occupies the only positive end  $\gamma_b$ , each such  $C_i$  only has ends on  $L_{t_*}$ . By a further decomposition, suppose  $C_i$  consists of  $Q_i$ -many sub-components lying entirely in the symplectization  $T^*L_{t_*} \setminus 0_{L_{t_*}}$ , denoted by  $\{u_i^j\}_{j=1, \dots, Q_i}$ . Each  $u_i^j$  has  $e_i^j$ -many negative ends and  $s_i^j$ -many positive ends. In particular,  $\sum_{j=1}^{Q_i} e_i^j = e_i$ . Similarly,  $C_i$  consists of  $R_i$ -many curves in  $E(a, b) \setminus U_g^* L_{t_*}$ , denoted by  $\{v_i^j\}_{j=1, \dots, R_i}$ . Each  $v_i^j$  has  $r_i^j$ -many negative ends on  $L_{t_*}$ , of type  $\{(-m_i^{j,l}, -n_i^{j,l})\}_{l=1, \dots, r_i^j}$ . See Figure 10 for an example of this decomposition of  $C_i$ . Note that  $\sum_{j=1}^{Q_i} s_i^j = (\sum_{j=1}^{R_i} r_i^j) + 1$  since there is one extra end matching with  $C_0$ . By Proposition 3.4(b) in [HO20], curves  $u_i^j$  in the symplectization have index  $\text{ind}(u_i^j) = 2s_i^j + e_i^j - 2$ . In addition, curves  $v_i^j$  in  $E(a, b) \setminus U_g^* L_{t_*}$  have index  $\text{ind}(v_i^j) = r_i^j - 2 + 2 \sum_{l=1}^{r_i^j} (m_i^{j,l} + n_i^{j,l})$  by the formula (11). Then by the index matching formula (15) again,

$$\begin{aligned} \text{ind}(C_i) - e_i &= \left( \sum_{j=1}^{R_i} \text{ind}(v_i^j) + \sum_{j=1}^{Q_i} \text{ind}(u_i^j) - \sum_{j=1}^{R_i} r_i^j \right) - e_i \\ &= \sum_{j=1}^{R_i} \left( r_i^j - 2 + 2 \sum_{l=1}^{r_i^j} (m_i^{j,l} + n_i^{j,l}) \right) \\ &\quad + \sum_{j=1}^{Q_i} (2s_i^j + e_i^j - 2) - \sum_{j=1}^{R_i} r_i^j - \sum_{j=1}^{Q_i} e_i^j \\ &= 2 \left( -R_i + \sum_{j=1}^{R_i} \sum_{l=1}^{r_i^j} (m_i^{j,l} + n_i^{j,l}) - Q_i + \sum_{j=1}^{Q_i} s_i^j \right). \end{aligned}$$

Now, for such a decomposition of  $C_i$  having genus 0, we can associate a tree to it by adding a vertex for each curve and each asymptotic end, and an edge between the vertex for a curve and each of its asymptotic end. We identify the two vertices corresponding to matching asymptotic ends. Since the Euler characteristic of a tree is always 1, we have

$$R_i + Q_i - \left( \sum_{j=1}^{Q_i} s_i^j - 1 \right) = 1, \quad \text{which implies } Q_i + R_i - \sum_{j=1}^{Q_i} s_i^j = 0.$$

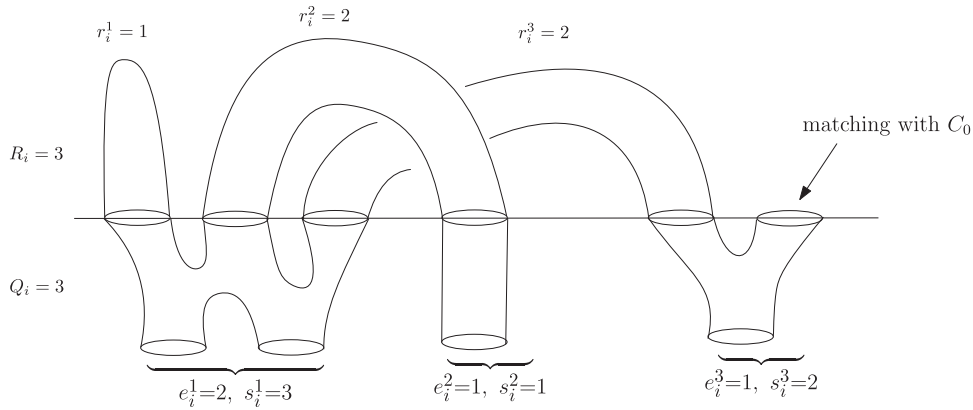


FIGURE 10. A decomposition of  $C_i$ .

Therefore, we obtain the following relation,

$$\text{ind}(C_i) - e_i = 2 \left( \sum_{j=1}^{R_i} \sum_{l=1}^{r_i^j} (m_i^{j,l} + n_i^{j,l}) \right).$$

Finally, summing over all  $i = \{1, \dots, k\}$ , we have

$$\begin{aligned} 2 \sum_{i=1}^k \sum_{j=1}^{l_i} (m_i^j + n_i^j) &= 2 \sum_{i=1}^k \sum_{j=1}^{R_i} \sum_{l=1}^{r_i^j} (m_i^{j,l} + n_i^{j,l}) \\ &= 2 \sum_{i=1}^k (\text{ind}(C_i) - e_i) \leq 0, \end{aligned}$$

where  $l_i = \sum_{j=1}^{R_i} r_i^j$  and the last step comes from (18). Thus, we complete the proof.  $\square$

A corollary of Lemma 4.3 is the following useful result. Denote by  $\mathcal{M}_{C_0}(t)$  the moduli space of the curve  $C_0$  in Lemma 4.3 (so, in particular, we are assuming the curves have a single positive end  $\gamma_b$ ) with moving boundary conditions on  $L_t$ . Recall that  $L_t$  is a Lagrangian isotopy which will cover a path  $\gamma(t) = (r(t), s(t))$  in the shape of  $E(a, b)$ . Denote by  $\text{area}_{C_0}(t)$  the (time-dependent) area of a curve in  $\mathcal{M}_{C_0}(t)$  with boundary on  $L_t$ , and similarly define  $\text{area}_C(t)$  where  $C$  is the curve we started from whose moduli space degenerated into  $C_{\text{lim}}$ . We note that these area formulas only depend on the moduli space of  $C$  or  $C_0$ , and actually only on the homology class of  $C_0$  and  $C$ . Thus, they are well defined even if the corresponding moduli space is empty and, in particular,  $\text{area}_C(t)$  is defined when  $t > t_*$ . Recall that  $t_* \in [0, 1]$  is the moment where  $C$  degenerates.

**PROPOSITION 4.4.** *Suppose  $r(t)/s(t)$  is non-increasing with respect the parameter  $t \in [0, 1]$  and the moduli space of  $C$  degenerates at time  $t_*$ . Then  $\text{area}_{C_0}(t) \leq \text{area}_C(t)$  for all  $t \in [t_*, 1]$ .*

*Proof.* We know that  $\text{area}_{C_0}(t_*) \leq \text{area}_{C_{\text{lim}}}(t_*) = \text{area}_C(t_*)$  since  $C_0$  is a component of  $C_{\text{lim}}$ , it suffices to prove the conclusion for  $t \in (t_*, 1]$ . Arguing by contradiction, suppose there exists

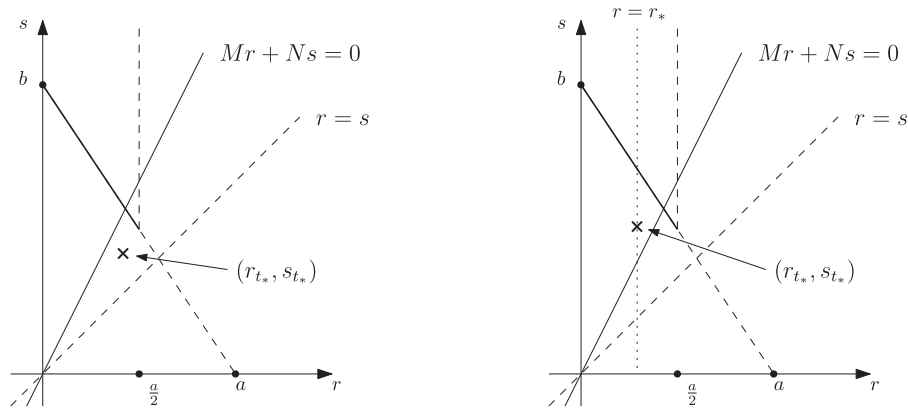


FIGURE 11. Relative position between  $(r_{t_*}, s_{t_*})$  and  $Mr + Ns = 0$ .

some  $t' \in (t_*, 1]$  such that  $\text{area}_{C_0}(t') > \text{area}_C(t')$ . Note that for any  $t \in [t_*, 1]$ , we have

$$\begin{aligned} \text{area}_C(t) &= \sum_{i=0}^k \text{area}_{C_i}(t) \\ &= \text{area}_{C_0}(t) + \left( \sum_{i=1}^k \sum_{j=1}^{l_i} m_i^j \right) r_t + \left( \sum_{i=1}^k \sum_{j=1}^{l_i} n_i^j \right) s_t, \end{aligned}$$

since, for homological reasons, curves in the symplectization contribute 0 to the area. For brevity, let  $M := \sum_{i=1}^k \sum_{j=1}^{l_i} m_i^j$  and  $N := \sum_{i=1}^k \sum_{j=1}^{l_i} n_i^j$ .

Arguing by contradiction, the relation  $\text{area}_{C_0}(t') > \text{area}_C(t')$  above implies that  $Mr_{t'} + Ns_{t'} < 0$ . Meanwhile, since at  $t = t_*$  each  $C_i$  for  $i \in \{1, \dots, k\}$  is a holomorphic curve, we have  $\sum_{i=1}^k \text{area}_{C_i}(t_*) > 0$ , which is equivalent to  $Mr_{t_*} + Ns_{t_*} > 0$ . Hence, since the function  $Mr_t + Ns_t$  is continuous with respect to time  $t$ , the intermediate value theorem implies that there exists  $t_\dagger \in (t_*, t')$  such that

$$Mr_{t_\dagger} + Ns_{t_\dagger} = 0. \tag{19}$$

There are two cases as follows, see Figure 11, depending on the relative position between  $(r_{t_*}, s_{t_*})$  and the line  $Mr + Ns = 0$ . In the left picture, the condition  $Mr_{t_*} + Ns_{t_*} > 0$  implies that the lower half plane given by the division of the line  $Mr + Ns = 0$  is the positive region. In particular, for any  $r = s (> 0)$ , we have

$$Mr + Nr > 0 \quad \text{which implies that } M + N > 0.$$

This contradicts Lemma 4.3. In the right picture, the condition  $Mr_{t_*} + Ns_{t_*} > 0$  implies that the upper half plane given by the division of the line  $Mr + Ns = 0$  is the positive region. By our hypothesis that  $r(t)/s(t)$  is non-increasing,  $\gamma|_{t > t_*}$  remains above the line  $Mr + Ns = 0$ , contradicting the existence of a  $t_\dagger$ . □

### 4.2 Proof of obstruction (I) in Theorems 2.11 and 2.12

*Outline.* We will trace the moduli space of the cylinder constructed in Lemma 4.1 under our Lagrangian isotopy. The idea is that if an isotopy as in obstruction (I) existed, then the area of any curves would decrease to 0, and hence as holomorphic curves have positive area we deduce there must be a degeneration to a non-trivial building. But by Proposition 4.4, we can then work

instead with a moduli space of curves from the limiting building whose areas would also decrease to 0, giving a contradiction.

*Proof.* Suppose by contradiction that a path  $\gamma = \{(r_t, s_t)\}_{t \in [0,1]}$  as in obstruction (I) admits a lift  $\{L_t\}_{t \in [0,1]}$ .

Denote by  $\mathcal{M}_1(t)$  the moduli space consisting of cylinders with positive end  $\gamma_b$  and negative end  $\gamma_{k,1}$  on the moving boundary  $L_t$ . By Lemma 4.1, we know that  $\mathcal{M}_1(0) \neq \emptyset$ , that is, there exists a  $C^{(1)} \in \mathcal{M}_1(0)$ . As before, the area of curves in  $\mathcal{M}_1(t)$  will be denoted by  $\text{area}_{C^{(1)}}(t)$ .

By (11) each  $C_t^{(1)} \in \mathcal{M}_1(t)$  has its index equal to

$$\begin{aligned} \text{ind}(C_t^{(1)}) &= (1 + 1 - 2) + 0 + (2 + 2k + 1) - (2(k + 1) + \frac{1}{2} - \frac{1}{2}) \\ &= (2k + 3) - (2k + 2) = 1. \end{aligned}$$

Hence, since  $\text{ind}(C_t^{(1)}) = 1 > -1 = 2 \cdot \text{genus}(C_t^{(1)}) - 2 + \#\Gamma_{\text{even}}$ , where  $\#\Gamma_{\text{even}}$  is the number of asymptotic ends with even CZ indices, curves in  $\mathcal{M}_1(t)$  are automatically regular (see Theorem 1 in [Wen10]). Thus,  $\mathcal{M}_1(t)$  is non-empty for an open subset of  $t \in [0, 1]$ .

Now suppose that the moduli space is compact. Then  $\mathcal{M}_1(0) \neq \emptyset$  together with automatic regularity implies that  $\mathcal{M}_1(1) \neq \emptyset$ . However, any curve  $C_1^{(1)} \in \mathcal{M}_1(1)$  has

$$\text{area}(C_1^{(1)}) = b - kr_1 - s_1 > 0, \quad \text{which means } \frac{r_1}{a} + \frac{s_1}{b} < 1. \tag{20}$$

This is in contradiction to our assumption that  $(r_1, s_1) \notin \mu(E(a, b))^+$ . Hence, the moduli space is not compact and we have a degeneration at some time  $t_* \in [0, 1]$ , that is, we have a holomorphic building  $C_{\text{lim}}^{(1)}$  which is a limit of curves  $C_n \in \mathcal{M}_1(t_n)$  with  $t_n \rightarrow t_*$ . The argument (20) implies that the degeneration point  $(r_{t_*}, s_{t_*})$  in fact occurs inside  $\text{int}(\mu(E(a, b))^+)$ .

By §3.3 in [HO20],  $C_{\text{lim}}^{(1)}$  contains a top-level curve, denoted by  $C^{(2)}$ , of index at least  $e$  and with  $e$  negative ends. We claim that  $C^{(2)}$  must have a positive end; we can then check that for index reasons it must be asymptotic to  $\gamma_b$ . Indeed, suppose not, then  $C^{(2)}$  can be thought of as a curve in  $\mathbb{C}^2 \setminus L_{t_*}$  and by Lemma 3.7 in [HO20] the curve  $C^{(2)}$  has area at least  $r_{t_*}$ . As any curve in  $\mathcal{M}_1(t_*)$  has area  $b - kr_{t_*} - s_{t_*}$ , we must then have  $r_{t_*} \leq \text{area}_{C^{(1)}}(t_*) < b - kr_{t_*} - s_{t_*}$ , which is equivalent to  $(k + 1)r_{t_*} + s_{t_*} < b$ , contradicting our assumption (I) on the path.

Denote by  $\mathcal{M}_2(t)$  the moduli space corresponding to the curve  $C^{(2)}$  above with the moving boundary condition on  $L_t$  for  $t \in [t_*, 1]$  and again we define  $\text{area}_{C^{(2)}}(t)$  to be the area of curves. If needed, consider  $\mathcal{M}_2(t)$  with extra marked points, so the resulting index is exactly equal to  $e$  (instead of at least  $e$ ). Then Proposition 4.4 implies that curves in the moduli space of  $C^{(2)}$  will not survive until  $t = 1$ . In fact, there must be a degeneration before time  $t_1$ , where  $\gamma|_{t=t_1}$  lies outside  $\mu(E(a, b))$ . Indeed, otherwise there will exist some curve denoted by  $C_{t_1}^{(2)} \in \mathcal{M}_2(t_1)$  that results in the following contradiction,

$$\text{area}(C_{t_1}^{(2)}) > 0 \quad \text{but } \text{area}_{C^{(2)}}(t_1) \leq \text{area}_{C^{(1)}}(t_1) \leq 0.$$

Therefore, the moduli space  $\mathcal{M}_2(t)$  is not compact over  $[t_*, 1]$  and it will degenerate again at some  $t_{**} \in (t_*, t_1)$ . We repeat the argument above by considering the limit building  $C_{\text{lim}}^{(2)}$  from a degeneration of  $C^{(2)}$  and pick the preferred top curve  $C^{(3)}$  as above. Next by Proposition 4.4 again, we will get a further degeneration, now within the time interval  $(t_{**}, t_1)$ , and so on.

We note that this process must terminate, and hence the desired contradiction is given by an inductive argument. To see this, suppose we have a sequence of  $C^{(k)}$  asymptotic to  $L_k \rightarrow L_\infty$ . Using Fukaya’s trick again there exists a family of global diffeomorphisms mapping our  $L_k$  to an  $\tilde{L}_\infty$ , where  $\tilde{L}_\infty$  lies very close to  $L_\infty$  but has rational area class, that is,  $\tilde{L}_\infty$  is Hamiltonian

isotopic to an  $L(\delta m, \delta n)$  with  $m, n \in \mathbb{N}$ . We may assume that the almost complex structures on the complement of the  $L_k$  push forward to tame almost complex structures on the complement of  $\tilde{L}_\infty$ . By construction, our  $C^{(k)}$  have a positive end, and in a degeneration of  $C^{(k)}$  the curve  $C^{(k+1)}$  is the only curve in the limiting building with an end on  $\partial E(a, b)$ . Therefore, the other top-level curves in the limit, when pushed forward to the complement of  $\tilde{L}_\infty$ , have area at least  $\delta$ . Hence, in the complement of  $\tilde{L}_\infty$ , the areas of the  $C^{(k)}$  decrease by at least  $\delta$  at each step, and so indeed our recursion is finite.  $\square$

**4.3 Proof of obstruction (I) in Theorem 2.13**

*Outline.* The proof of the obstruction to the path lifting in the polydisks  $P(c, d)$  is similar to the proof in balls and integral ellipsoids. The only variation is that we start from a curve that is different from that from Lemma 4.1 or Remark 4.2.

*Proof.* Suppose by contradiction that path  $\gamma = \{(r_t, s_t)\}_{t \in [0,1]}$  admits a lift  $\{L_t\}_{t \in [0,1]}$ . Compactify  $P(c, d)$  to  $S^2(c) \times S^2(d)$  with two factors having areas  $c$  and  $d$ . Denote by  $\mathcal{M}_1(t)$  the moduli space consisting of finite energy planes that intersect  $S^2(c) \times \{\infty\}$  only once (i.e. it is of bidegree  $(0, 1)$ ) and has its negative asymptotic end  $\gamma_{(0,1)}$  on the moving boundary  $L_t$  for  $t \in [0, 1]$ . The moduli space  $\mathcal{M}_1(0)$  is non-empty since we can simply write out (the image of) a curve  $C^{(1)}$  explicitly as follows:

$$C^{(1)} = \{(z, w) \in \mathbb{C}^2 \mid z = \text{constant}, \pi|w|^2 > d\},$$

and by (13)  $\text{ind}(C^{(1)}) = -1 + 2 \cdot 2 + 2 \cdot (-1) = 1$ , plus the automatic regularity can be verified.

Now, suppose that the moduli space is compact, then  $\mathcal{M}_1(1) \neq \emptyset$ . Any curve  $C_1^{(1)} \in \mathcal{M}_1(1)$  satisfies  $\text{area}(C_1^{(1)}) = d - s_1 > 0$ , which contradicts our assumption that  $(r_1, s_1) \notin \mu(P(c, d))^+$ . Hence, we have a degeneration at some time  $t_* \in [0, 1]$  with a limit curve a holomorphic building  $C_{\text{lim}}^{(1)}$ . By § 3.3 in [HO20],  $C_{\text{lim}}^{(1)}$  contains a top-level curve  $C^{(2)}$  of index at least  $e$  with  $e$  negative ends. This curve  $C^{(2)}$  intersects  $S^2(c) \times \{\infty\}$  since otherwise, by [HO20, Lemma 3.7], it has area at least  $r_{t_*}$  and then

$$r_{t_*} \leq \text{area}_{C^{(2)}}(t_*) < d - s_{t_*}$$

which contradicts our assumption (I) on the path.

Denote by  $\mathcal{M}_2(t)$  the moduli space corresponding to the curve  $C^{(2)}$  above with moving boundary on  $L_t$  for  $t \in [t_*, 1]$ . It is readily checked that the same conclusion in Lemma 4.3 holds if we replace the assumption ‘contains the positive end  $\gamma_b$ ’ with ‘intersects  $S^2(c) \times \{\infty\}$ ’. Then Proposition 4.4, whose argument only involves areas, implies that  $\mathcal{M}_2(t)$  is not compact, so it will degenerate again at  $t_{**} \in (t_*, t_1)$  where  $t_1$  is the first time that  $\gamma$  intersects the line segment  $\{(r, d) \in \mathbb{R}_{>0}^2 \mid 0 < r < c/2\}$ . The rest of the proof goes exactly the same as that in § 4.2, and thus we get the desired conclusion.  $\square$

**5. Construction of path lifting**

**5.1 Path lifting criterion**

In this section we construct our path lifts. The main result is the following theorem giving a Hamiltonian isotopy with controlled support between an inclusion and a *rolled up* Lagrangian. The domains of interest are the  $Q(a, b)$  defined here.

DEFINITION 5.1. The domain  $Q(a, b) \subset \mathbb{C}^2$  is defined by

$$Q(a, b) = \Omega_{q(a,b)} := \{(z, w) \in \mathbb{C}^2 \mid (\pi|z|^2, \pi|w|^2) \in q(a, b)\}$$

where

$$q(a, b) = \left\{ (x, y) \in \mathbb{R}^2 \mid 0 \leq x \leq 2a - \frac{ay}{a+b}, 0 \leq y \leq a+b \right\}, \tag{21}$$

a quadrilateral region in  $\mathbb{R}^2$ .

**THEOREM 5.2.** *Let  $0 < a < b$  and  $\epsilon > 0$ . Then there exists a Hamiltonian isotopy of the Lagrangian tori denoted by  $\{L_t\}_{t \in [0,1]}$  with  $L_0 = L(a, b)$  such that the following conclusions hold:*

- (1) *for every  $t \in [0, 1]$ , the Lagrangian  $L_t \subset Q(a + \epsilon, b + \epsilon)$ ;*
- (2)  *$L_1 \subset Q(a + \epsilon, a + \epsilon)$ .*

*Remark 5.3.* The existence of a Hamiltonian diffeomorphism with the property (2) has been established in [HZ21, Theorem 6.3], which, in turn, relied on §6 in [HO20]. These proofs however essentially wrote down the torus  $L_1$  and then applied general methods to show the  $L_1$  to be Hamiltonian isotopic to  $L(a, b)$ , hence losing control of the support of the isotopy. The improvement here is that the whole isotopy is fairly explicit, allowing us to add conclusion (1) in Theorem 5.2. This condition is, of course, vital for the quantitative study of isotopies in the current paper.

*Proof of Theorem 5.2.* The following lemma will be used. It is well known and can be proved by applying a symplectic conjugation mapping the disks  $D(a)$  to rectangles  $(0, 1) \times (0, a)$ . Let  $D(c)$  denote an open round disk in the plane, centered at the origin and with area  $c$ .

**LEMMA 5.4.** *Let  $\epsilon > 0$ . There exists a function  $G$  with compact support in  $D(2a + \epsilon)$  and  $0 \leq G \leq a + \epsilon$  such that the corresponding Hamiltonian flow  $\phi_G^t$  satisfies  $\phi_G^t(D(a)) \subset D((1+t)a + \epsilon)$  and  $\phi_G^1(D(a)) \cap D(a) = \emptyset$ .*

We use coordinates  $(z, w)$  on  $\mathbb{C}^2$ . We define a product Lagrangian torus  $\tilde{L}(a, b)$  in  $\mathbb{C}^2$  by

$$\tilde{L}(a, b) := \partial D(a) \times \partial([0, 1] \times [0, b]),$$

where  $[0, 1] \times [0, b]$  is a rectangle in  $w$ -plane. Let  $w = x + \sqrt{-1}y$ . Note that a smoothing of  $\tilde{L}(a, b)$  is symplectomorphic to our standard product by a symplectomorphism on  $\mathbb{C}$  that interchanges the disk  $D(b)$  with the rectangle  $[0, 1] \times [0, b]$  in the  $w$ -plane.

Consider a product Hamiltonian function

$$H(z, w) = \chi(y) \cdot G(z),$$

where  $\chi : [0, a + \epsilon] \rightarrow [0, 1]$  is a smooth function, extended by zero outside  $[0, a + \epsilon]$ , such that for a sufficiently small  $\delta > 0$  we have:

- (i)  $\chi|_{[0,\delta]} = 1$ ,  $\chi|_{[a+\epsilon-\delta,a+\epsilon]} = 0$ , and  $\chi|_{[2\delta,a+\epsilon-2\delta]}$  is linear of slope  $-1/(a + \epsilon + \delta)$ ;
- (ii)  $\chi|_{[\delta,2\delta]}$  is concavely decreasing and  $\chi|_{[a+\epsilon-2\delta,a+\epsilon-\delta]}$  is convexly decreasing.

See Figure 12 for the pictures of  $\chi(y)$  and  $-\chi'(y)$ . The function  $G(z)$  is defined by Lemma 5.4.

By the product rule we have  $dH(z, w) = \chi'(y)G(z) dy + \chi(y) dG(z)$ . Using the standard symplectic structure on  $\mathbb{C}^2$ , that is,  $\omega_{\text{std}} = \omega_{\text{std},\mathbb{C}} + dx \wedge dy$ , we can write down the Hamiltonian vector field  $X_H$  (via the Hamiltonian equation  $-dH = \iota_{X_H} \omega_{\text{std}}$ ), namely

$$X_H(z, w) = -\chi'(y)G(z) \frac{\partial}{\partial x} + \chi(y)X_{G(z)}(z),$$

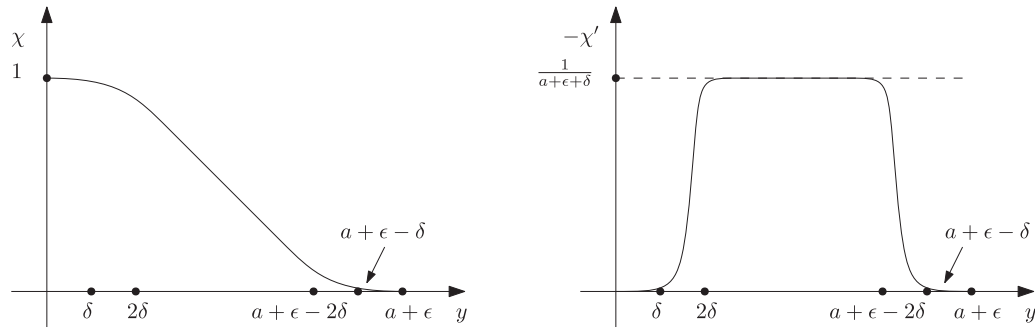


FIGURE 12. Graphs of  $\chi(y)$  and  $-\chi'(y)$ .

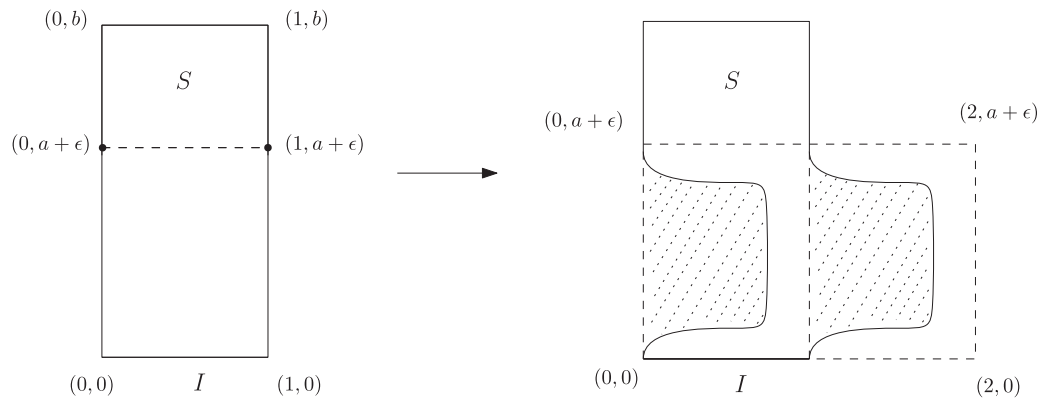


FIGURE 13. Behavior of  $\phi_H^1(L(a, b))$  on the  $w$ -plane.

where  $X_{G(z)}$  is the Hamiltonian vector field generated by the function  $G(z)$  above with respect to  $\omega_{\text{std}, \mathbb{C}}$ . Therefore, the resulting Hamiltonian diffeomorphism of  $H$  is

$$\phi_H^t(z, w) = (\phi_{\chi \cdot G}^t(z), (x - t\chi'(y)G(z), y)). \tag{22}$$

Now, apply the Hamiltonian diffeomorphism  $\phi_H^1$  to  $\tilde{L}(a, b)$ , and Figure 13 shows a schematic picture of how the projection to the  $w$ -plane changes (indicated by the shaded part). For later use, we label the rectangle  $S := [0, 1] \times [a + \epsilon, b]$ . By our choice of  $\epsilon$  and  $\delta$  as above,

$$\max_{\tilde{L}(a,b)} \{-\chi'(y)G(z)\} \leq \frac{a + \epsilon}{a + \epsilon + \delta} < 1.$$

Therefore, the bottom part of the rectangle which is moved by  $\phi_H^1$  is contained in the rectangle  $[0, 2] \times [0, a + \epsilon]$  and touches neither the line  $x = 1$  nor  $x = 2$ .

On the other hand, for the behavior on the  $z$ -plane, there are two extreme cases.

- (a) For  $w \in I$ , i.e.  $w = (x, 0)$  for  $x \in [0, 1]$ , since  $\chi(0) = 1$ , the first factor in (22) is simply  $\phi_G^1(z)$  which by definition displaces  $\partial D(a)$  (since it displaces  $D(a)$ ).
- (b) For  $w$  near  $S$ , where  $S$  is the upper part of the rectangle as in Figure 13, since  $\chi(y) = 0$ , the second factor in (22) is identity, so  $\partial D(a)$  stays the same.

Next, we also consider a Hamiltonian isotopy  $\{\psi_t\}_{t \in [0,1]}$  on the  $w$ -plane that wraps the region  $S$  around the deformed  $w$ -projection to overlap the rectangle  $[0, 1] \times [0, a + \epsilon]$ , see Figure 14. Although on the  $w$ -plane, there are intersection points of  $\psi_t|_S(S)$  with the line segment  $I$ , by our construction, viewed in four dimensions there will be no extra intersections. Indeed, for any

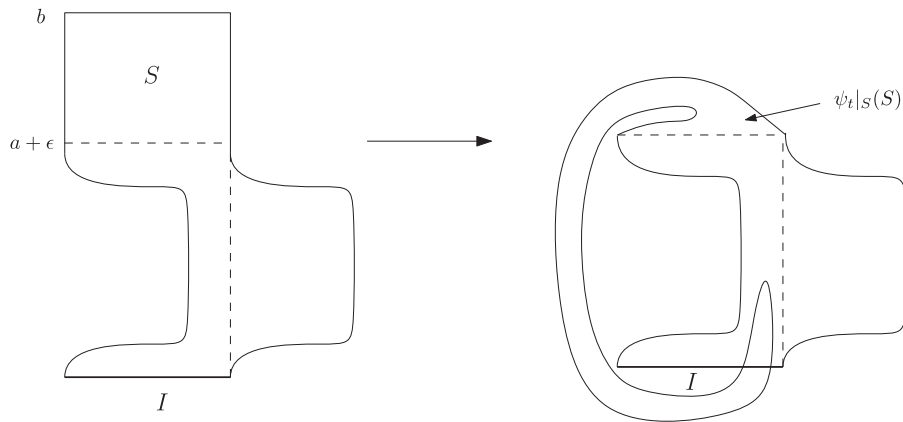


FIGURE 14. Wrap the region  $S$ .

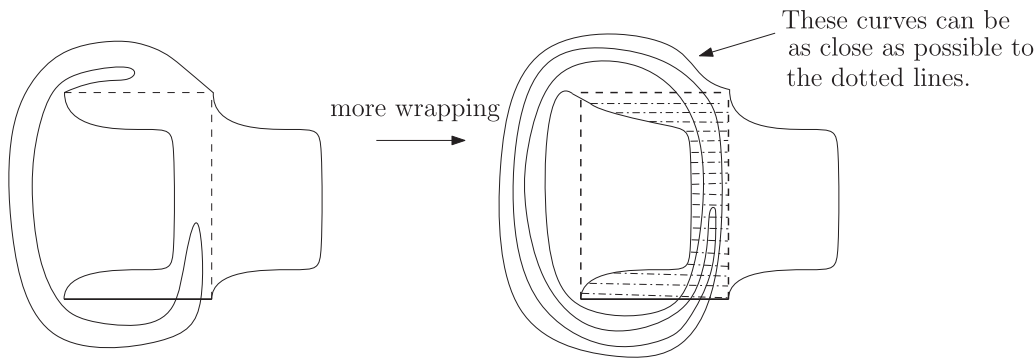


FIGURE 15. More wrappings.

point  $(z, w)$  with  $w$  near  $S$ , the corresponding  $z \in D(a)$ , but by case (a) above for any point  $(z, w)$  with  $w \in I$ , the corresponding  $z$  lies in  $\phi_G^1(D(a))$  which is disjoint from  $D(a)$ . Continuing this wrapping construction as shown in Figure 15, we can wrap all of  $S$  into the shaded region Figure 15, which is a subset of  $[0, 1] \times [0, a + \epsilon]$ , union with an arbitrarily small neighborhood, say of width  $\delta \ll \epsilon$ , of the sides  $[0, 1] \times \{0\}$ ,  $\{0\} \times [0, a + \epsilon]$  and  $[0, 1] \times \{a + \epsilon\}$ .

The Hamiltonian isotopy of interest is the image, under a symplectomorphism  $\mathbb{1} \times \Phi$ , of the concatenation of the two constructions above,

$$\{\phi_H^t(\tilde{L}(a, b))\}_{t \in [0, 1]} \# \{\psi_t(\phi_H^1(\tilde{L}(a, b)))\}_{t \in [0, 1]}. \tag{23}$$

Here  $\Phi$  is a symplectomorphism of the  $w$ -plane that maps

- (i)  $[-\delta, 2] \times [-\delta, a + \epsilon + \delta] \cup [0, 1] \times [a, y]$  into  $D(a + y + 3\epsilon)$  for  $y \geq a + \epsilon$ ; and
- (ii) each horizontal rectangle  $[-\delta, 2] \times [-\delta, y]$  into  $D(2y + \epsilon)$  for  $y \in [0, a + \epsilon]$ .

See Figure 16 for a layer-by-layer picture of such a map  $\Phi$  for part (ii). The existence of such symplectomorphisms follows Lemma 3.1.5 in the book [Sch05].

Note that both  $\Phi([0, 1] \times [0, b])$  and  $D(b)$  lie inside  $D(a + b + 3\epsilon)$ . Therefore, without loss of generality, we may assume  $\Phi([0, 1] \times [0, b]) = D(b)$ , that is, our isotopy starts at the standard product  $L(a, b)$ .

We need to keep track of the moment image  $(\pi|z|^2, \pi|w|^2)$  along the Hamiltonian isotopy and have the following observations.

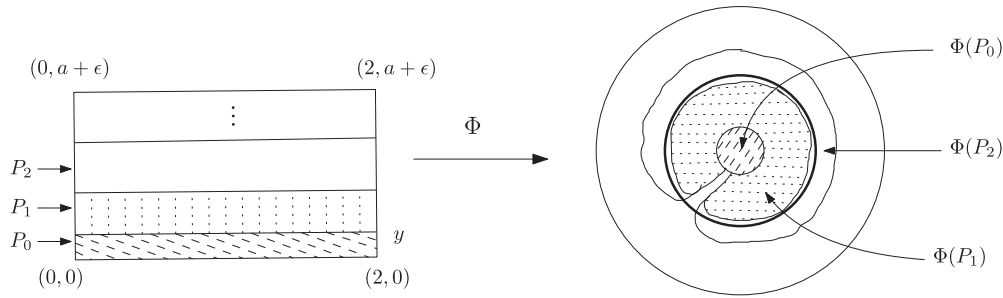


FIGURE 16. The map  $\Phi$  on  $[0, 2] \times [0, a + \epsilon]$ .

*Case  $\alpha$ .* Let  $(z, w) = (z, (x, y)) \in \tilde{L}(a, b)$  with  $y \in [0, a + \epsilon]$ . We denote the image of  $(z, w)$  under  $\phi_H^t$  by  $(z', w')$ , and this point is described by (22). In particular, the  $y$  coordinate is invariant under the flow. Hence, under the symplectomorphism  $\mathbb{1} \times \Phi$ , we get the relation

$$\pi|\Phi(w')|^2 \leq 2y + \epsilon \quad \text{and} \quad z' \in D(2a - y + 4\epsilon). \tag{24}$$

For the bound on  $\pi|\Phi(w')|^2$  we are applying condition (ii) on  $\Phi$ . For the condition on  $z'$ , by (22) we note that  $z' = \phi_{\chi_G}^t(z) = \phi_G^{t\chi}(z)$  where  $z \in D(a)$ , since  $G$  is independent of time. But

$$\chi(y) \leq \frac{a + \epsilon - y}{a + \epsilon + \delta} < 1 - \frac{y}{a + \epsilon + \delta}$$

and so by Lemma 5.4

$$z' \in D\left(a + a - \frac{ay}{a + \epsilon + \delta} + \epsilon\right) \subset D(2a - y + 4\epsilon)$$

as required.

The relation (24) yields

$$2a - y + 4\epsilon \leq 2a - \frac{\pi|\Phi(w')|^2 - \epsilon}{2} + 4\epsilon \leq 2a - \frac{\pi|\Phi(w')|^2}{2} + 5\epsilon,$$

and then, importantly,

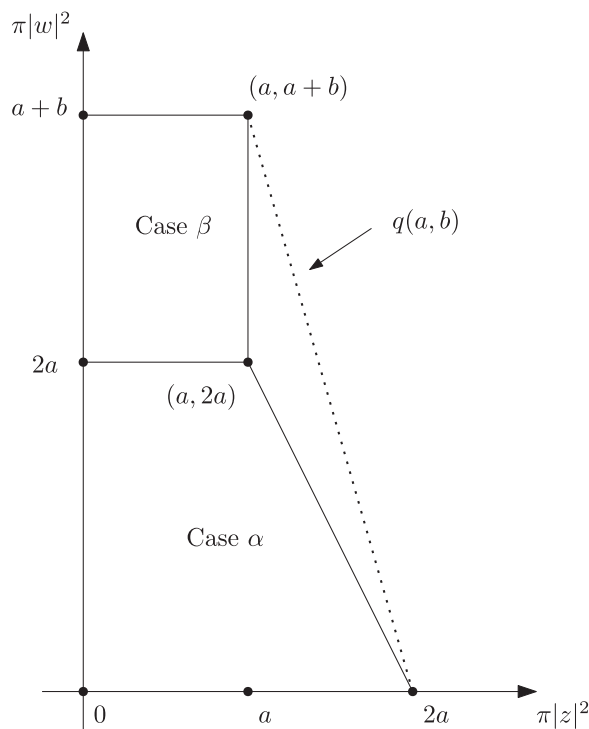
$$\pi|z'|^2 \leq 2a - y + 4\epsilon \leq 2a - \frac{\pi|\Phi(w')|^2}{2} + 5\epsilon.$$

Such points  $(z', w')$  are then fixed by the flow  $\psi_t$ .

*Case  $\beta$ .* Let  $(z, w) = (z, (x, y)) \in \tilde{L}(a, b)$  with  $y \in [a + \epsilon, b]$ . Such points are fixed by  $\phi_H^t$ , and the flow of  $\psi_t$  fixes the  $z$  coordinate and leaves the  $w$  coordinate inside an  $\epsilon$  neighborhood of  $[0, 1] \times [0, b]$ . This region is mapped close to  $D(a + b)$  by  $\Phi$ , using property (i).

Therefore, we obtain a Lagrangian isotopy with its moment image lying in regions corresponding to either case  $\alpha$  or case  $\beta$  as above. The following graph illustrates these regions, for

brevity, when  $\epsilon \rightarrow 0$ .



The union of these regions is contained in an arbitrarily small neighborhood of the quadrilateral region defined by  $q(a, b) \subset \mathbb{R}^2$  in our hypothesis. We note in Case  $\beta$  the points  $\psi_1(z, w)$  lie in an  $\epsilon$  neighborhood of  $D(a) \times [0, 1] \times [0, a]$ . Therefore, by property (i) of  $\Phi$ , the image under  $\mathbb{1} \times \Phi$  lies close to  $D(a) \times D(2a)$  and the moment image is described only by the lower trapezium in the graph above. In other words, at  $t = 1$  the moment image of the Lagrangian isotopy (23) lies in an arbitrarily small neighborhood of  $q(a, a)$ . Hence, we complete the proof.  $\square$

In constructing lifts, our strategy will be to divide  $\gamma$  into segments, and on each segment lift either by inclusions or by the rolled up Lagrangian embeddings described in Theorem 5.2. The following lemma says that a Hamiltonian isotopy is enough to piece these lifts together. In other words, we are free to concatenate paths with endpoints lying in the same path component of a fiber.

LEMMA 5.5. *Let  $\gamma : [0, 2] \rightarrow \mathbb{R}^2$  and  $L_t, 0 \leq t \leq 1$  and  $M_t, 1 \leq t \leq 2$  be smooth families of Lagrangian tori in  $\mathcal{L}(X)$  such that  $\mathcal{P}(L_t) = \gamma(t)$  and  $\mathcal{P}(M_t) = \gamma(t)$  and  $L_1$  is Hamiltonian isotopic to  $M_1$  in  $X$ , that is,  $L_1$  and  $M_1$  lie in the same component of the fiber over  $\gamma(1)$ . Then  $\gamma(t)$  has a smooth lift  $N_t$  with  $N_t = L_t$  for  $t < 1 - \epsilon$  and  $N_t = M_t$  for  $t > 1 + \epsilon$ .*

*Proof.* Let  $\Phi_t \in \text{Ham}(X)$  be a Hamiltonian flow with  $\Phi_0 = \text{I}$  and  $\Phi_1(L_1) = M_1$ . First we replace  $L_t$  by  $\tilde{L}_t = \Phi_{f(t)}(L_t)$  where  $f(t) = 0$  for  $t < 1 - \epsilon$  and  $f(1) = 1$ . Then  $\tilde{L}_t$  and  $M_t$  together give a continuous lift of  $\gamma(t)$ .

To smooth a possible corner at  $\tilde{L}_1 = M_1$  we first identify a neighborhood of  $M_1$  in  $X$  with a neighborhood of the zero section in  $T^*\mathbb{T}^2$ . Then Lagrangian tori near  $M_1$  can be identified with the graphs of closed 1 forms  $\alpha = r d\theta_1 + s d\theta_2 + dg$  where  $\theta_1, \theta_2$  are coordinates on  $\mathbb{T}^2$  and  $g(\theta_1, \theta_2)$  is a smooth function. Here  $r$  and  $s$  are uniquely defined, and  $g$  is also uniquely defined if we insist that  $\int g = 0$ . Moreover, we may assume that up to a translation the map  $\mathcal{P}$  is given by

$\mathcal{P}(\text{gr}(\alpha)) = (r, s)$ . Now finding a smooth lift just requires replacing the family of  $g$  corresponding to  $\tilde{L}_t$  and  $M_t$  by a smooth family of functions. □

Let  $X_\Omega$  be a toric domain in  $\mathbb{R}^4$  with moment image  $\Omega$ . Recall that a Type-I path is a path that entirely lies in  $\Omega^+ := \Omega \cap \{r \leq s\}$  and any other path with starting point in  $\Omega^+$  is a Type-II path. The following corollary of Theorem 5.2 provides our key sufficient condition to lift a general path.

**COROLLARY 5.6** (Path lifting criterion). *Let  $X_\Omega \subset \mathbb{R}^4$  be a toric domain and let  $\gamma = \{(r_t, s_t) \mid r_t < s_t\}_{t \in [0, T]}$  be an oriented path in  $\text{Sh}_H^+(X_\Omega)$ . Then  $\gamma$  lifts to  $\mathcal{L}(X_\Omega)$  if it can be decomposed as a concatenation of sub-paths of Type-I and Type-II such that each Type-II path has the following property. Suppose the Type-II sub-path has domain  $[t_0, t_1] \subset [0, 1]$ . Then there exists a  $t_* \in (t_0, t_1]$  and  $\epsilon > 0$  such that:*

- (II-i)  $\gamma|_{[t_0, t_*]} \subset \Omega^+$  but  $\gamma|_{[t_*, t_1]} \not\subset \Omega^+$ ;
- (II-ii)  $q(r_{t_*} + \epsilon, s_{t_*} + \epsilon) \subset \text{int}(\Omega)$ , and, if  $t_1 \neq T$ , then also  $q(r_{t_1}, s_{t_1}) \subset \text{int}(\Omega)$ ;
- (II-iii)  $q(r_t + \epsilon, r_t + \epsilon) \subset \text{int}(\Omega)$  for all  $t \in [t_*, t_1]$ .

*Proof of Corollary 5.6.* By Example 2.10, any Type-I sub-path and the part  $\gamma|_{[0, t_*]}$  of a Type-II sub-path always lifts via product tori, so we need to consider the part  $\gamma|_{[t_*, t_1]}$  of a Type-II sub-path, which is not entirely contained in  $\Omega^+$ . By condition (II-iii) these segments lift using the family of rolled up embeddings described by Theorem 5.2. To do this, starting from the Lagrangian  $\psi_1(\phi_H^1(L(a, b)))$  as in Figure 15, we can continuously change the areas of the disk  $D(a)$  in the  $z$ -plane to be the given  $r_t$  and the height  $b$  of the rectangle in Figure 13 to be the given  $s_t$ , for  $t \in [t_*, t_1]$ . The construction still applies since  $r_t < s_t$  for all  $t \in [0, 1]$ , and the resulting Lagrangian  $L_t$  is Hamiltonian isotopic to the product Lagrangian torus  $L(r_t, s_t)$  since we can run the constructions  $\psi_t$  and  $\phi_H^t$  above in reverse (cf. the requirement of the condition  $a < b$  for the constructions above). Moreover, the image of  $L_t$  lies in an arbitrarily small neighborhood of  $Q(r_t, r_t)$

It remains to adjust things so that our Lagrangian embeddings match at the endpoints of the segments, and by Lemma 5.5 it is enough to show these embeddings are Hamiltonian isotopic in  $X_\Omega$ . But at an endpoint  $t_1$  say, Theorem 5.2 gives such an isotopy from the product to the rolled up torus with support in a neighborhood of  $Q(r_{t_1}, s_{t_1})$ , and by condition (II-ii) we have that  $Q(r_{t_1} + \epsilon, s_{t_1} + \epsilon) \subset X_\Omega$ . In this way, we get the desired conclusion. □

**5.2 Proof of criterion (II) in Theorems 2.11, 2.12, and 2.13**

5.2.1 *Proof of Theorem 2.11(II).* We will show that a path  $\gamma$  as described in Theorem 2.11(II) satisfies the lifting criterion in Corollary 5.6. Assuming the path is not of Type-I, it is already of Type-II and no decomposition into sub-paths is necessary. Our  $t_*$  is given, and condition (II-i) follows since the path is Type-II.

Recall that the moment image  $\mu(B^4(R))$  is the right triangle  $\Delta(R, R)$  in the  $(r, s)$  plane with vertices  $(0, 0)$ ,  $(R, 0)$  and  $(0, R)$ . Condition (II-ii) in Corollary 5.6,  $q(r_{t_*}, s_{t_*}) \subset \text{int}(\Delta(R, R))$ , is equivalent to the condition that the vertex  $(r_{t_*}, r_{t_*} + s_{t_*})$  lies strictly below the hypotenuse of  $\Delta(R, R)$ . Since the equation of the hypotenuse is  $r + s = R$ , the condition is

$$r_{t_*} + (r_{t_*} + s_{t_*}) < R$$

as given in Theorem 2.11.

Similarly, condition (II-iii) in Corollary 5.6 is equivalent  $r_t < R/3$  for  $t \in [0, T]$ . Thus, we complete the proof. □

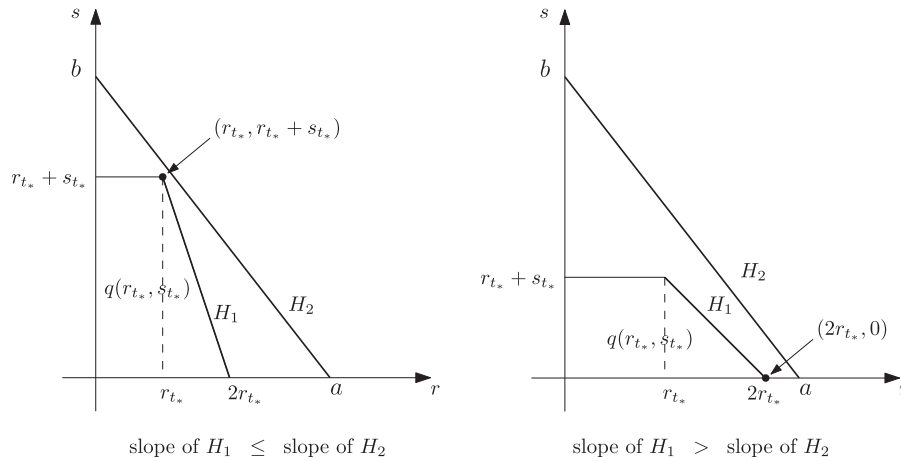


FIGURE 17. Comparisons of slopes.

5.2.2 *Proof of Theorem 2.12(II)*. As for Theorem 2.11(II) we need to check that the conditions in Theorem 2.11(II) imply the path  $\gamma$  satisfies the conditions in Corollary 5.6. These are automatic if  $\gamma$  is of Type-I, otherwise we think of  $\gamma$  as a single path of Type-II.

Recall that  $\mu(E(a, b))$  is the right triangle  $\Delta(a, b)$  with vertices  $(0, 0)$ ,  $(a, 0)$ , and  $(0, b)$ . We have two cases for condition (II-ii) of Corollary 5.6, due to the comparison between the slope of the hypotenuse of this triangle and the slope of the hypotenuse of the quadrilateral region  $q(r_{t_*}, s_{t_*})$  (see Figure 17). The slope  $H_1$  is  $-(r_{t_*} + s_{t_*})/r_*$  while the slope of  $H_2$  is  $-k = -b/a$ . Then for the first case where  $-(r_{t_*} + s_{t_*})/r_* \leq -k$  (which is equivalent to  $(k - 1)r_{t_*} \leq s_{t_*}$ ), we have  $q(r_{t_*}, s_{t_*}) \subset \text{int}(\Delta(a, b))$  if and only if the vertex  $(r_{t_*}, r_{t_*} + s_{t_*})$  lies strictly below the hypotenuse  $H_2$ . Since the line represented by  $H_2$  is  $r/a + s/b = 1$ , we require

$$\frac{r_{t_*}}{a} + \frac{r_{t_*} + s_{t_*}}{b} < 1,$$

which, writing  $a = b/k$ , is equivalent to  $(k + 1)r_{t_*} + s_{t_*} < b$  as in Theorem 2.12(II-ii-1). Similarly, for the second case where  $-(r_{t_*} + s_{t_*})/r_* > -k$  (which is equivalent to  $(k - 1)r_{t_*} > s_{t_*}$ ), we have  $q(r_{t_*}, s_{t_*}) \subset \text{int}(\Delta(a, b))$  if and only if the vertex  $(2r_*, 0)$  lies strictly on the left of  $(a, 0)$ , that is,  $2r_{t_*} < a$  as in Theorem 2.12(II-ii-2).

For condition (II-iii) in Corollary 5.6, note that the slope of the hypotenuse  $H_1$  of the quadrilateral region  $q(r_t, r_t)$  is always  $-2$  which is no greater than the slope of the hypotenuse  $H_2$  (since we assume  $k \geq 2$ ). Therefore, the condition is equivalent to  $2r_t < a$  as in Theorem 2.12. Thus, we complete the proof.  $\square$

5.2.3 *Proof of Theorem 2.13(II)*. Recall that the moment image  $\mu(P(c, d))$  is the rectangle  $\square(c, d)$  with vertices  $(0, 0)$ ,  $(c, 0)$ ,  $(0, d)$ , and  $(c, d)$ . Condition (II-ii) in Corollary 5.6,  $q(r_{t_*}, s_{t_*}) \subset \text{int}(\square(a, b))$ , is equivalent to the vertex  $(2r_*, 0)$  lying on the left of  $(c, 0)$  and the height  $r_* + s_*$  being lower than  $d$ . In other words, we require

$$r_* < \frac{c}{2} \quad \text{and} \quad r_* + s_* < d.$$

Similarly, condition (II-iii),  $q(r_t, r_t) \subset \text{int}(\square(c, d))$ , is determined by the vertex  $(2r_t, 0)$ , and requires  $r_t < c/2$  for  $t \in [t_*, T]$ . As these conditions are fulfilled by the path in Theorem 2.13 we complete the proof as before.  $\square$

**5.3 Proof of Theorems 2.5, 2.6, and 2.7**

Now, we are ready to see how these path lifting criteria easily imply the existence of knotted Lagrangian tori in  $B^4(R)$ ,  $E(a, b)$ , and  $P(c, d)$ . We will give the proof of these three theorems simultaneously.

For any area classes  $(r, s)$  in the given region (4) or (5) or (6), consider the path  $\gamma = \{\gamma(t)\}_{t \in [0,1]}$  with

$$\gamma(t) = (r, (1 - t)s + ts_*)$$

where  $(r, s_*) \notin \Delta(R, R)$  or  $(r, s_*) \notin \Delta(a, b)$  or  $(r, s_*) \notin \square(c, d)$ , respectively. By Theorem 2.1, we know  $\gamma \subset \text{Sh}_H^+(B^4(R))$ ,  $\gamma \subset \text{Sh}_H^+(E(a, b))$ , and  $\gamma \subset \text{Sh}_H^+(P(c, d))$ , respectively. Choose a path  $\tilde{\gamma}$  that sits entirely inside  $\Delta(R, R)^+$  or  $\Delta(a, b)^+$  or  $\square(c, d)^+$  such that the whole of  $\tilde{\gamma}$  satisfies condition (II-iii) of Theorem 2.11, 2.12, or 2.13, respectively, and such that  $\tilde{\gamma}$  starts at a point satisfying condition (II-ii) and ends at  $(r, s)$ . Now, consider the concatenation

$$\tilde{\gamma} \# \gamma \in \text{Sh}_H^+(B^4(R)) \text{ or } \text{Sh}_H^+(E(a, b)) \text{ or } \text{Sh}_H^+(P(c, d)).$$

Then by condition (II) in Theorem 2.11, 2.12, or 2.13, respectively, we know  $\tilde{\gamma} \# \gamma$  lifts to a Lagrangian isotopy of tori. In particular, there exists a Lagrangian sub-isotopy which projects via  $\mathcal{P}$  to  $\gamma$ , starting from  $(r, s)$ . If there do not exist any knotted Lagrangian tori in the fiber  $\mathcal{P}^{-1}((r, s))$ , then up to Hamiltonian isotopy in  $B^4(R)$  or  $E(a, b)$  or  $P(c, d)$ , we can assume this sub-isotopy starts from the product Lagrangian torus  $L(r, s)$ . Then, by Definition 2.9,  $\gamma$  lifts and it contradicts condition (I) in Theorem 2.11, 2.12, or 2.13, respectively. Thus, we complete the proof. □

*Remark 5.7.* We note that the paths  $\tilde{\gamma}$  used in the proof above are examples of paths in the shape with non-unique lifts. Indeed, the proof shows that the lift of  $\tilde{\gamma} \# \gamma$  at the endpoint of  $\tilde{\gamma}$  is a knotted Lagrangian torus, but as it lies in the moment image  $\tilde{\gamma}$  also admits a lift to a family of product tori.

**6. Hamiltonian knottedness in  $\mathbb{C}P^2$**

In this section, we give the proof of Theorem 2.8.

*Proof of Theorem 2.8.* By the wrapping construction from Theorem 5.2, we find a Lagrangian torus, denoted by  $L_{r,s}$ , with area classes  $(r, s)$  and lying inside  $B^4(R)$ , so also lying inside  $\mathbb{C}P^2$ . To distinguish  $L_{r,s}$  from the fiber  $L(r, s)$  inside  $\mathbb{C}P^2$ , we will use the  $\Psi$ -invariant considered in [STV18]. This computes the minimal area of Maslov 2 holomorphic disks with boundary on the corresponding Lagrangian torus. By Theorem 4.4 in [STV18],  $\Psi(L)$  is well-defined for any embedded Lagrangian tori in  $\mathbb{C}P^2$ , in particular, it is independent of the almost complex structure and invariant under the Hamiltonian isotopy. We will obtain the desired conclusion by showing that  $\Psi(L(r, s)) \neq \Psi(L_{r,s})$ .

For the fiber  $L(r, s)$ , with respect to the standard almost complex structure  $J_0$  on  $\mathbb{C}P^2$ , there are three (standard) Maslov 2  $J_0$ -holomorphic disks with boundaries on  $L(r, s)$ , denoted by  $D_1, D_2, D_3$ , intersecting the three edges of moment image  $\mu(\mathbb{C}P^2(R))$  once for each and with areas

$$\text{area}(D_1) = r, \quad \text{area}(D_2) = s, \quad \text{area}(D_3) = R - r - s.$$

Since  $(r, s)$  satisfies  $2r + s > R$ , we have  $R - r - s < r$ , that is,  $\text{area}(D_3) < \text{area}(D_1) < \text{area}(D_2)$ . In particular, by definition,  $\Psi(L(r, s)) \leq R - r - s$ .

On the other hand, for the wrapped Lagrangian torus  $L_{r,s}$ , we claim that  $\Psi(L_{r,s}) \geq r$ . This leads to the desired conclusion that  $\Psi(L_{r,s}) > \Psi(L(r, s))$ , in particular, not equal. To obtain this

claim, we will divide the Maslov 2 disks  $D$  with boundary on  $L_{r,s}$  into the following two classes:

$$I = \{D \mid D \cap S_\infty = \emptyset\} \quad \text{and} \quad II = \{D \mid D \cap S_\infty \neq \emptyset\}.$$

For the family I, since  $L_{r,s}$  is Hamiltonian isotopic to  $L(r, s)$  in  $\mathbb{C}^2$ , a computation of the  $\Psi$  invariant in  $\mathbb{C}^2$  implies that any holomorphic disk  $D$  will have  $\text{area}(D) \geq r$ . For the family II, we will prove it by contrapositive as follows.

Suppose there exists  $D \in II$  with intersection number  $d \geq 1$  but with  $\text{area}(D) < r$ . Let  $(-m, -n)$  be the homology class of the boundary. Then the Maslov 2 condition gives

$$m + n + 3d = 1.$$

and the area is

$$\begin{aligned} \text{area}(D) &= dR + rm + sn = dR + r(-3d + 1 - n) + sn \\ &= d(R - 3r) + r + n(s - r). \end{aligned}$$

By our hypothesis  $r < R/3$  and  $d \geq 1$ , we see that if  $\text{area}(D) < r$ , then  $n \leq -1$ .

Now, similarly to the proof of Theorem 2.5, consider the following straight line path  $\gamma(t) = (r, (1 - t)s + ts_*)$  in  $\text{Sh}_H^+(B^4(R))$ , for  $t \in [0, 1]$  but with sufficiently large  $S$ . Note that this path lifts to a Lagrangian isotopy  $\{L_t\}_{t \in [0,1]}$ , starting from  $L_{r,s}$ . Viewing  $\{L_t\}_{t \in [0,1]}$  inside  $\mathbb{C}P^2$ , if the corresponding family of holomorphic disks  $D_t$  persists, then, as the degree is fixed (since the  $L_t$  lie in the ball disjoint from the line at infinity) and  $n \leq -1$ , we will have  $\text{area}(D_1) = d(R - 3r) + r + n(s_* - r)$  which is negative for  $s_*$  sufficiently large and a contradiction.

Alternatively the family of disks is not compact, and we have bubbling into the union of a Maslov 0 and a Maslov 2 disk. As  $\text{area}(D_t)$  is a decreasing function of  $t$  the Maslov 2 component will also have area less than  $r$ , and the calculation above shows that it will be asymptotic to a class  $(-m_1, -n_1)$  with  $n_1 < 0$ . Thus, the new family of Maslov 2 disks again will have decreasing area and cannot persist until time  $t = 1$  (the degree can only decrease after a degeneration by positivity of intersection). Arguing by induction, we have a contradiction as in § 4.2.

In this way, we have shown that any Maslov 2 disk  $D \in II$  must have area at least  $r$ . Together with the argument for the disks in the family I, we obtain the desired claim, and thus complete the proof. □

*Remark 6.1.* Proposition 2.8 also follows directly from Corollary 6.7 in [STV18] on the straight line path of the shape invariant. More precisely, if  $L_{r,s}$  is Hamiltonian isotopic to the fiber  $L(r, s)$  inside  $\mathbb{C}P^2$ , then Corollary 6.7 in [STV18] proves that the longest straight line starting from  $L_{r,s}$  stops at the boundary of  $\mu(\mathbb{C}P^2)$ , while our straight line path chosen in the proof of Theorem 2.8 above can go (vertically) far beyond  $\mu(\mathbb{C}P^2)$ . This provides the requested contradiction. We include the argument above for completeness as the Corollary 6.7 ultimately relies on similar considerations.

The holomorphic disks in the above proof could be substituted for finite energy curves as in § 4.1. However, degenerations of holomorphic disks are slightly simpler to analyze.

### 7. An exotic example

As explained in the introduction, path lifting can be subtle for various reasons. In this section, we illustrate this complexity via an exotic example. Consider  $\gamma_1$  and  $\gamma_2$  in  $\text{Sh}_H^+(E(a, b))$  with  $k := b/a = 3$  shown in Figure 18. In the left picture,  $\gamma_1$  when viewed with either orientation lifts from  $\text{Sh}_H^+(E(a, b))$  to a closed loop of Lagrangians. The picture indicates the concatenation

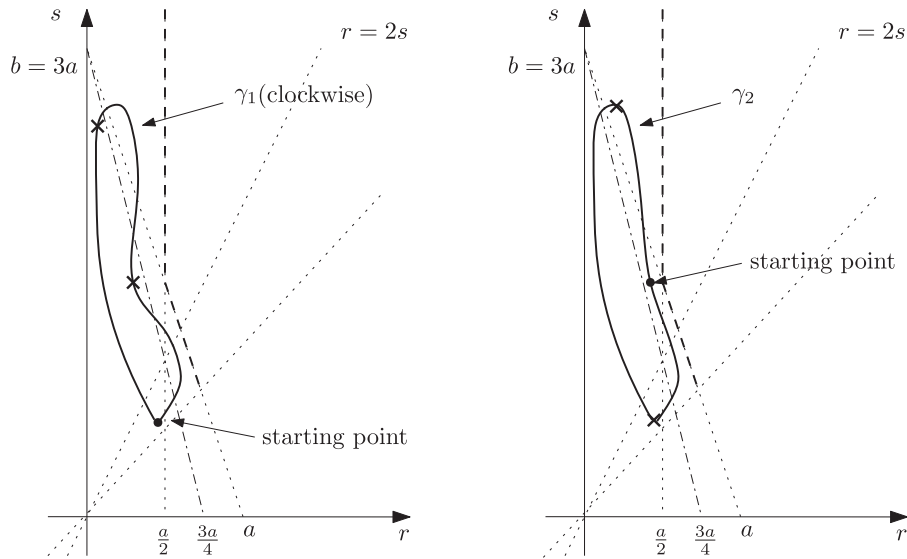


FIGURE 18. Path  $\gamma_1$  lifts, but path  $\gamma_2$  lifts only viewed clockwise.

points (two places labeled by crosses), and the sub-paths change types from Type-I to Type-II, then back to Type-I (see § 2.2).

On the other hand, in the right picture, the path  $\gamma_2$  is a small perturbation of  $\gamma_1$  as a geometric path. If we view it clockwise, then this is an example showing a certain *monodromy* phenomenon. Note that  $\gamma_2$  lifts by condition (II) in Theorem 2.12 and the picture indicates the concatenation point as the lower cross. Explicitly, it starts from a Type-I sub-path, followed by a Type-II sub-path. This Type-II sub-path ends at the same point as the starting point. Meanwhile, since this Type-II sub-path never comes back to the ‘flexible’ region below the line  $4r + s = b$ , as in the left picture, the Lagrangian torus at the endpoint is not a product torus. Therefore, this closed loop  $\gamma_2$  lifts but not as a *loop* of Lagrangian tori.

Finally, if we view  $\gamma_2$  counterclockwise, i.e. considering its reverse path  $\bar{\gamma}_2$ , then it does *not* lift. Otherwise, the sub-path from the starting point to the upper cross will lift, and it violates the obstruction, i.e. condition (I) in Theorem 2.12. This shows that the orientation in the path lifting also matters.

### 8. Obstructions to symplectic embeddings

In this section, we will demonstrate how to use path lifting to obstruct symplectic embeddings between domains in  $\mathbb{R}^4$ . Let us start from the following result.

PROPOSITION 8.1. *Let  $X, Y$  be two toric domains in  $\mathbb{R}^4$ , and let  $\gamma$  be a path in  $\text{Sh}_H^+(X)$  that lifts to a Lagrangian isotopy of tori in  $\mathcal{L}(X)$ , denoted by  $\{L_t\}_{t \in [0, T]}$ . If there exists a symplectic embedding  $X \hookrightarrow Y$  such that the image of  $L_0$  is unknotted in  $Y$ , then  $\gamma$  lies in  $\text{Sh}_H^+(Y)$  and lifts to  $\mathcal{L}(Y)$ .*

*Proof.* The first conclusion comes directly from Proposition 7.1 in [HZ21]. It suffices to prove the second conclusion. Suppose  $\gamma = \{(r_t, s_t) \in \text{Sh}_H^+(X) \mid t \in [0, T]\}$ . Since  $\gamma$  lifts to  $\mathcal{L}(X)$ , the corresponding Lagrangian isotopy of tori  $L = \{L_t\}_{t \in [0, T]}$  satisfies  $\mathcal{P}(L_t) = (r_t, s_t)$ . Suppose the symplectic embedding  $X \hookrightarrow Y$  is  $\phi$ , and consider the Lagrangian isotopy

$$\phi(L) = \{\phi(L_t)\}_{t \in [0, T]} \subset \mathcal{L}(Y).$$

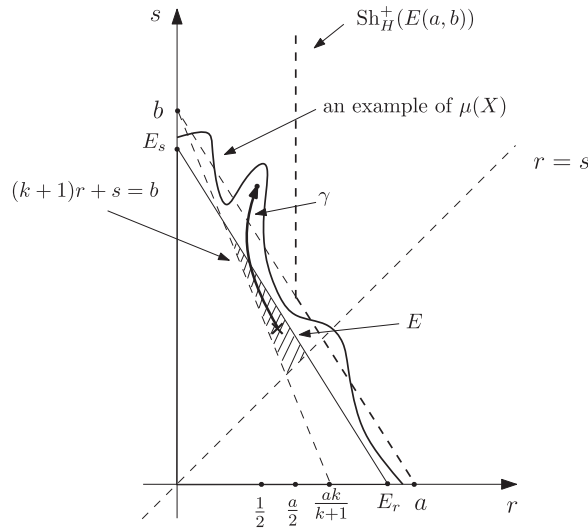


FIGURE 19. The obstruction is given by the bold path.

Similarly to Proposition 7.1 in [HZ21], we know  $\mathcal{P}(\phi(L_t)) = (r_t, s_t)$  for any  $t \in [0, T]$ . Meanwhile, by assumption,  $\phi(L_0)$  is unknotted in  $Y$ , so by definition there exists a Hamiltonian isotopy  $\Psi = \{\Psi_t\}_{t \in [0, T]}$  of  $Y$  such that  $\Psi_1(\phi(L_0)) = L(r_0, s_0)$ . Then the following Lagrangian isotopy of tori in  $Y$ ,

$$\tilde{L} = \{\Psi_1(\phi(L_t))\}_{t \in [0, T]} \subset \mathcal{L}(Y)$$

is the desired lift of  $\gamma$  in  $\text{Sh}_H^+(Y)$  since  $\text{Ham}(Y)$  preserves the fibers of  $\mathcal{P}$ . In other words,  $\gamma \subset \text{Sh}_H^+(Y)$  lifts to  $\mathcal{L}(Y)$  by  $\tilde{L}$ , and we complete the proof.  $\square$

### 8.1 Proof of Theorem 2.16

We will only give the proof of criterion (1); criteria (2) and (3) can be proved in a similar manner.

For the given  $(r, s)$ , consider the *straight line* path  $\gamma$  starting at  $(r, s)$  and ending at  $(0, x)$ . Since it is a straight line with  $2r + s > R$  and  $x > R$ , this path  $\gamma$  lies entirely outside the ‘flexible’ region below the line  $2r + s = R$ . Meanwhile, again  $x > R$  implies that  $\gamma$  will escape the moment image  $\Delta(R, R)$  eventually. Then, on the one hand, since  $\gamma$  lies entirely in the moment image  $\Delta(1, x)$ , Example 2.10 implies that it lifts to  $\mathcal{L}(E(1, x))$ . On the other hand, if  $\phi(L(r, s))$  is unknotted under the embedding  $\phi : E(1, x) \hookrightarrow B^4(R)$ , then Proposition 8.1 implies that  $\gamma \subset \text{Sh}_H^+(B^4(R))$  and it lifts as well. However, this contradicts Theorem 2.11(I). Therefore, we obtain the desired conclusion.

### 8.2 Proof of Theorem 2.21

Assumption (ii) implies that  $\gamma$  lifts to  $\mathcal{L}(X)$  since  $\gamma$  lies entirely in  $\mu(X)^+$ . In particular, the starting point  $(r_0, s_0)$  can be realized as the inclusion of the product Lagrangian torus  $L(r_0, s_0) \hookrightarrow X$ . Now, suppose that there exists a symplectic embedding  $\phi : X \hookrightarrow E(a, b)$ . By the first condition in assumption (i), we have

$$L(r_0, s_0) \subset E \xrightarrow{i} X \xrightarrow{\phi} E(a, b),$$

where  $i$  is the inclusion. Replacing  $E$  by a slightly smaller closed ellipsoid, Corollary 1.6 in [McD09] proves that the space of symplectic embeddings from  $E$  to  $E(a, b)$  denoted by  $\text{Emb}(E, E(a, b))$  is connected, and then the condition  $E \subset E(a, b)$  implies that every symplectic embedding from  $E$  to  $E(a, b)$  is isotopic to the inclusion. In particular, the product Lagrangian torus  $L(r_0, s_0) \subset E$  is unknotted under the symplectic embedding  $\phi \circ i$ . Then Proposition 8.1 implies that  $\gamma \subset \text{Sh}_H^+(E(a, b))$  and it lifts to  $\mathcal{L}(E(a, b))$ . This contradicts Theorem 2.12(I), and therefore we obtain the desired contradiction. Figure 19 shows a schematic picture of this proof, where  $E = E_{\Delta(E_r, E_s)}$  and the moment image  $\Delta(E_r, E_s)$  is shown as the triangle with vertices  $(0, 0)$ ,  $(E_r, 0)$ , and  $(0, E_s)$ , the image  $\mu(X)$  is described via the profile curve (without arrow), and the obstruction is given by  $\gamma$ , shown as the bold path (with arrow).

ACKNOWLEDGEMENTS

This work was completed when the second author held the position of CRM-ISM Postdoctoral Research Fellow at CRM, University of Montreal, and the second author thanks this institute for its warm hospitality. We also thank an anonymous referee for a thorough report.

CONFLICTS OF INTEREST

None.

Appendix A

This section verifies the following result, up to a rescaling by  $a/(k + 1)$ , that was used in Example 2.18(2).

PROPOSITION A.1. *For any  $k \in \mathbb{N}$ ,  $E(k, (k + 1)^2) \hookrightarrow E(k + 1, k(k + 1))$ .*

From Hutchings’ work [Hut11] and McDuff’s work [McD11], there exists a complete characterization of four-dimensional ellipsoid embeddings, that is,

$$E(c, d) \hookrightarrow E(a, b) \quad \text{if and only if} \quad \mathcal{N}(c, d)_k \leq \mathcal{N}(a, b)_k. \tag{A.1}$$

Here,  $\mathcal{N}(a, b)$  denotes an infinite sequence of numbers consisting of all the non-negative linear combinations  $ma + nb$  (for  $m, n \in \mathbb{Z}_{\geq 0}$ ) in a non-decreasing order (with repetitions), and  $\mathcal{N}(a, b)_k$  is the  $k$ th entry in  $\mathcal{N}(a, b)$ , similarly to  $\mathcal{N}(c, d)_k$  and  $\mathcal{N}(c, d)$ . In fact, there exists a nice geometric description of  $\mathcal{N}(a, b)$  (see §3.3 in [Hut11]). Denote by  $\Delta_{a,b}(t)$  the closed right triangle in  $\mathbb{R}^2$  with vertices  $(0, 0)$ ,  $(t/a, 0)$ , and  $(0, t/b)$  for  $t \geq 0$ , and denote

$$\mathcal{R}_{a,b}(t) := \#\{\Delta_{a,b}(t) \cap \mathbb{Z}_{\geq 0}^2\}. \tag{A.2}$$

Then the characterization (A.1) is equivalent to the statement that  $E(c, d) \hookrightarrow E(a, b)$  if and only if  $t_2 \leq t_1$  whenever  $\mathcal{R}_{c,d}(t_2) = \mathcal{R}_{a,b}(t_1)$ . Since  $\mathcal{R}_{a,b}(t)$  and  $\mathcal{R}_{c,d}(t)$  are non-decreasing functions of  $t$ , (A.1) is further equivalent to the following statement:

$$E(c, d) \hookrightarrow E(a, b) \quad \text{if and only if} \quad \mathcal{R}_{c,d}(t) \geq \mathcal{R}_{a,b}(t) \quad \text{for all } t \geq 0. \tag{A.3}$$

We emphasize that the statement (A.1) (as well as (A.3)), are not always easy to verify. However, the equivalent statement (A.3) has the advantage that some elementary geometry propositions can be applied. For instance, in terms of counting lattice points, the well-known Pick’s theorem is very useful. Explicitly, for any polygon with integer vertices and without holes,

$$\#\{\text{interior lattice points}\} + \frac{\#\{\text{boundary lattice points}\}}{2} = \text{area} + 1. \tag{A.4}$$

The proof of Proposition A.1 turns out to be a nice combination of the criterion (A.3) and Pick’s theorem (A.4).

*Proof of Proposition A.1.* By (A.3), it suffices to show  $\mathcal{R}_{k,(k+1)^2}(t) \geq \mathcal{R}_{k+1,k(k+1)}(t)$  for any  $t \geq 0$ . We will prove this in two steps. First, we have the following result.

LEMMA A.2. For any  $k \in \mathbb{N}$  and  $A \in \mathbb{Z}_{\geq 0}$ , we have

$$\mathcal{R}_{k,(k+1)^2}(Ak(k+1)) = \mathcal{R}_{k+1,k(k+1)}(Ak(k+1)) = \frac{1}{2}kA(A+1) + (A+1).$$

*Proof of Lemma A.2.* For the right triangle  $\Delta_{k+1,k(k+1)}(Ak(k+1))$ , its  $x$ -intercept is  $t/a = Ak(k+1)/(k+1) = Ak$  and its  $y$ -intercept is  $t/b = Ak(k+1)/k(k+1) = A$ , where both  $Ak, k \in \mathbb{Z}_{\geq 0}$ . Then Pick’s theorem applies, and (A.4) implies that

$$\mathcal{R}_{k+1,k(k+1)}(Ak(k+1)) = \frac{A^2k}{2} + 1 + \frac{\#\{\text{boundary lattice points}\}}{2}.$$

Meanwhile, by elementary counting,  $\#\{\text{boundary lattice points}\} = 2A + Ak$ . Therefore, we get the desired conclusion for  $\mathcal{R}_{k+1,k(k+1)}(Ak(k+1))$ .

For the right triangle  $\Delta_{k,(k+1)^2}(Ak(k+1))$ , let us introduce the following notation,

$$c = \left\lfloor \frac{Ak}{k+1} \right\rfloor = \frac{Ak}{k+1} - \frac{C}{k+1},$$

where  $C \in \mathbb{N}$  and  $0 \leq C \leq k$ , and

$$b = \left\lfloor \frac{A}{k+1} \right\rfloor = \frac{A}{k+1} - \frac{B}{k+1},$$

where  $B \in \mathbb{N}$  and  $0 \leq B \leq k$ . Here is a useful observation.

CLAIM A.3. Either  $B = C = 0$  or  $B + C = k + 1$ . In the second case we have  $\lfloor Bk/(k+1) \rfloor = B - 1$ .

*Proof of Claim A.3.* First we note that if  $B = 0$ , then  $A$  is a multiple of  $k + 1$  and so also  $C = 0$ . Henceforth, then we suppose  $B > 0$ .

We have

$$\frac{Ak}{k+1} = kb + \frac{kB}{k+1}.$$

Therefore, we can write  $kB = m(k+1) + C$  where  $m \geq 0$  is an integer. More explicitly,  $m = \lfloor kB/(k+1) \rfloor$ . As  $B > 0$  we have  $m < B$ , but if  $m \leq B - 2$ , then

$$C = kB - m(k+1) \geq kB - (k+1)(B-2) = 2k - B + 2 \geq k + 2,$$

a contradiction. Hence,  $m = B - 1$  and we get  $C = kB - (k+1)(B-1) = k + 1 - B$ . It is easy to check that  $B + C = k + 1$  implies  $\lfloor Bk/(k+1) \rfloor = B - 1$ , and, therefore, we get the desired claim.  $\square$

Next, we will count lattice points in  $\Delta_{k,(k+1)^2}(Ak(k+1))$ . Divide  $\Delta_{k,(k+1)^2}(Ak(k+1))$  into two parts as in Figure A.1, one small triangle  $\Delta_{\text{small}}$  and one trapezoid  $P_{\text{trapezoid}}$ . Here the horizontal line  $y = bk$  is excluded from  $\Delta_{\text{small}}$  and considered as part of  $P_{\text{trapezoid}}$ . In the case when  $B = C = 0$  we make no division and  $P_{\text{trapezoid}}$  can be used to denote our original closed triangle  $\Delta_{k,(k+1)^2}(Ak(k+1))$ . The way we cut in Figure A.1 guarantees that there are no lattice points on the hypotenuse of  $\Delta_{\text{small}}$  except possibly at the endpoints. Indeed, since the slope of  $\Delta_{k,(k+1)^2}(Ak(k+1))$  is  $-k/(k+1)^2$ , moving from the vertex  $(A(k+1), 0)$  to the vertex

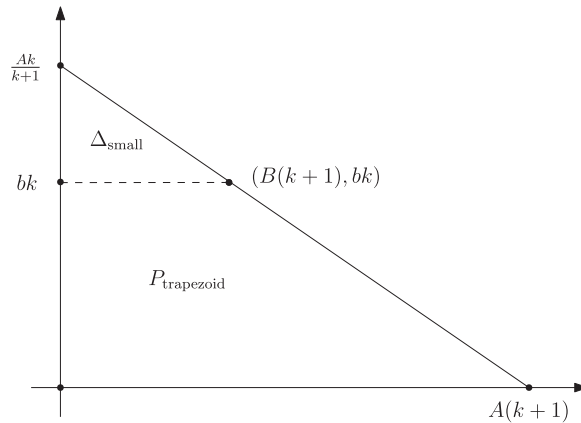


FIGURE A.1. A division of  $\Delta_{k,(k+1)^2}(Ak(k+1))$ .

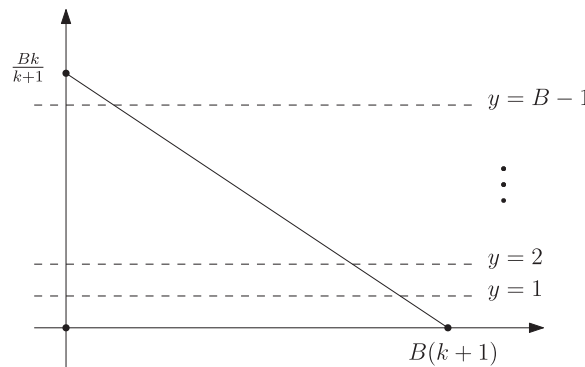


FIGURE A.2. Line-by-line counting in  $\Delta_{\text{small}}$ .

$(0, Ak/(k+1))$ , only when the  $x$  coordinate decreases by a multiple of  $(k+1)^2$  can we see a lattice point on the hypotenuse of  $\Delta_{k,(k+1)^2}(Ak(k+1))$ . There are at most  $\lfloor A/(k+1) \rfloor$ -many non-zero multiples of  $(k+1)^2$  in the interval  $[0, A(k+1)]$  and the smallest is

$$A(k+1) - \left\lfloor \frac{A}{k+1} \right\rfloor (k+1)^2 = \left( \frac{A}{k+1} - \left\lfloor \frac{A}{k+1} \right\rfloor \right) (k+1)^2 = B(k+1).$$

Meanwhile, it is easy to verify that the corresponding  $y$ -coordinate is  $bk$ .

Now  $P_{\text{trapezoid}}$  is a polygon with integer vertices and without holes. Hence, Pick's theorem applies, and (A.4) implies that

$$\# \left\{ \begin{array}{l} \text{lattice points} \\ \text{in } P_{\text{trapezoid}} \end{array} \right\} = \frac{bk(k+1)(A+B)}{2} + 1 + \frac{\#\{\text{boundary lattice points}\}}{2}.$$

Moreover, by an elementary counting,  $\#\{\text{boundary lattice points}\} = (A+B+b)(k+1)$ . Therefore,

$$\# \left\{ \begin{array}{l} \text{lattice points} \\ \text{in } P_{\text{trapezoid}} \end{array} \right\} = \frac{bk(k+1)(A+B)}{2} + 1 + \frac{(A+B+b)(k+1)}{2}. \tag{A.5}$$

We note this formula applies in all cases, including when  $B=0$  and  $P_{\text{trapezoid}}$  is a triangle.

For the small triangle  $\Delta_{\text{small}}$ , up to an integer shift (explicitly shifted down by  $bk$ ), it suffices to consider the following triangle in Figure A.2. In particular, the top horizontal line intersecting

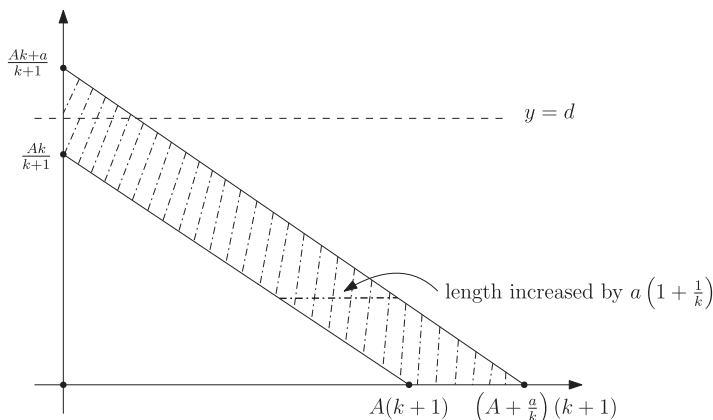


FIGURE A.3. Count additional lattice points in the shaded region.

the triangle and with integer intercept is  $y = \lfloor Bk/(k+1) \rfloor$ . In the case when the triangle is non-trivial, that is  $B \neq 0$ , Claim A.3 above says that  $\lfloor Bk/(k+1) \rfloor = B - 1$ . There are no lattice points in the interior of the hypotenuse of the triangle in Figure A.2, and for each  $\ell \in \{1, \dots, B - 1\}$ , the intersection of the line  $y = \ell$  with this triangle admits  $(B(k+1) - \ell(k+2))$ -many lattice points on its the interior. Then

$$\begin{aligned} \# \left\{ \begin{array}{l} \text{lattice points} \\ \text{in } \Delta_{\text{small}} \end{array} \right\} &= \sum_{\ell=1}^{B-1} (B(k+1) - \ell(k+2)) \\ &= B(B-1)(k+1) - \frac{B(B-1)(k+2)}{2} \\ &= \frac{B(B-1)k}{2}. \end{aligned} \tag{A.6}$$

(Again we note this formula remains valid in the case when  $B = 0$ , that is, the triangle is empty and there are no lattice points.)

Hence, by summing up the lattices points in  $P_{\text{trapezoid}}$  (as in (A.5)) and in  $\Delta_{\text{small}}$  (as in (A.6)), we have

$$\begin{aligned} \mathcal{R}_{k,(k+1)^2}(Ak(k+1)) &= \# \left\{ \begin{array}{l} \text{lattice points} \\ \text{in } P_{\text{trapezoid}} \end{array} \right\} + \# \left\{ \begin{array}{l} \text{lattice points} \\ \text{in } \Delta_{\text{small}} \end{array} \right\} \\ &= \frac{bk(k+1)(A+B)}{2} + 1 + \frac{(A+B+b)(k+1)}{2} + \frac{B(B-1)k}{2} \\ &= \frac{1}{2}kA(A+1) + (A+1), \end{aligned}$$

where the final step comes from a series of simplifications using the relation  $B = A - b(k+1)$ . Thus, we complete the proof of Lemma A.2.  $\square$

Suppose now that  $t = Ak(k+1) + s$  where  $0 < s < k(k+1)$ . Observe that the graph of  $\mathcal{R}_{k+1,k(k+1)}(t)$  is horizontal with jumps when  $s = a(k+1)$  for integers  $a$ . Thus, to establish our proposition, we may assume  $s = a(k+1)$  with  $1 \leq a \leq k-1$ . Then we have

$$\mathcal{R}_{k+1,k(k+1)}((Ak+a)(k+1)) - \mathcal{R}_{k+1,k(k+1)}(Ak(k+1)) = (A+1)a. \tag{A.7}$$

It remains to estimate  $\mathcal{R}_{k,(k+1)^2}((Ak+a)(k+1)) - \mathcal{R}_{k,(k+1)^2}(Ak(k+1))$ , and we aim to obtain at least  $(A+1)a$  as in (A.7) (see Figure A.3). To this end, we use the same notation as above,

but also introduce

$$d = \left\lfloor \frac{Ak + a}{k + 1} \right\rfloor = \frac{Ak + a}{k + 1} - \frac{D}{k + 1},$$

where  $D \in \mathbb{N}$  and  $0 \leq D \leq k$ . Note that  $d - c \leq 1$ . Moreover:

- (i) if  $d = c$ , then  $a \leq k + 1 - C$  and  $D = C + a$ ;
- (ii) if  $d = c + 1$ , then  $D = C + a - (k + 1)$ .

When condition (i) is satisfied the triangle intersects no new rows with integer intercepts; this is automatically the case when  $B = 0$ . When condition (ii) is satisfied, the new triangle intersects  $y = d$  and the row contains

$$1 + \left\lfloor \frac{D}{k + 1} \frac{(k + 1)^2}{k} \right\rfloor = 1 + \left\lfloor \frac{(k + 1)D}{k} \right\rfloor \tag{A.8}$$

lattice points. Meanwhile, the lengths of the other rows increase by  $a(1 + 1/k)$ , so we count the number of additional lattice points as

$$a + (a + 1) + \dots + (a + 1) + a + \dots + a + \dots,$$

where the  $(a + 1)$  terms come in blocks of length  $a$  and the  $a$  terms in blocks of length  $k - a$ . Therefore, depending whether the sum ends with  $(a + 1)$  (if  $c - kb \leq a$ ) or  $a$  terms (if  $c - kb \geq a + 1$ ), we have

$$\# \left\{ \begin{array}{l} \text{additional} \\ \text{points} \end{array} \right\} = \begin{cases} a + (k + 1)ab + (c - kb)(a + 1) & \text{if } c - kb \leq a, \\ a + (k + 1)ab + a(c - kb + 1) & \text{if } c - kb \geq a + 1. \end{cases}$$

It is easy to obtain the desired  $(A + 1)a$ -many additional lattice points when  $B = C = 0$ . If not, then Claim A.3 implies that  $b + c = A - 1$  and  $c - kb = B - 1$ , and a further simplification gives

$$\# \left\{ \begin{array}{l} \text{additional} \\ \text{points} \end{array} \right\} = \begin{cases} aA + B - 1 & \text{if } c - kb \leq a, \\ (A + 1)a & \text{if } c - kb \geq a + 1. \end{cases}$$

Therefore, it suffices to focus on the case where  $c - kb \leq a$ .

If  $d = c$ , then by item (i) above,  $D = C + a = k + 1 - B + a$ , which implies that  $B - 1 = a + k - D \geq a$ . Thus, we get at least  $(A + 1)a$ -many additional lattice points as required. If  $d = c + 1$ , then we have an extra row so the cardinality of the additional points in total is  $aA + B + \lfloor (k + 1)D/k \rfloor$  by (A.8). Item (ii) above implies that  $D = a - B$  and then we have

$$aA + B + \left\lfloor \frac{(k + 1)D}{k} \right\rfloor = aA + a - D + \left\lfloor \frac{(k + 1)D}{k} \right\rfloor \geq (A + 1)a.$$

Therefore, we complete the proof of Proposition A.1. □

*Remark A.4.* Since  $\text{Vol}(E(k, k + 1)^2) = \text{Vol}(E(k + 1, k(k + 1))) = k(k + 1)^2/2$ , the symplectic embedding guaranteed by Proposition A.1 is volume-filling.

REFERENCES

BEH<sup>+</sup>03 F. Bourgeois, Y. Eliashberg, H. Hofer, K. Wysocki and E. Zehnder, *Compactness results in symplectic field theory*, *Geom. Topol.* **7** (2003), 799–888; [MR 2026549](#).

BEP12 L. Buhovsky, M. Entov and L. Polterovich, *Poisson brackets and symplectic invariants*, *Selecta Math. (N.S.)* **18** (2012), 89–157; [MR 2891862](#).

Cha83 M. Chaperon, *Quelques questions de géométrie symplectique*, *Astérisque* **105** (1983), 231–249; [MR 728991](#).

- Che96 Yu. V. Chekanov, *Lagrangian tori in a symplectic vector space and global symplectomorphisms*, Math. Z. **223** (1996), 547–559; [MR 1421954](#).
- CS10 Y. Chekanov and F. Schlenk, *Notes on monotone Lagrangian twist tori*, Electron. Res. Announc. Math. Sci. **17** (2010), 104–121; [MR 2735030](#).
- CM18 K. Cieliebak and K. Mohnke, *Punctured holomorphic curves and Lagrangian embeddings*, Invent. Math. **212** (2018), 213–295; [MR 3773793](#).
- CG19 D. Cristofaro-Gardiner, *Symplectic embeddings from concave toric domains into convex ones*, J. Differential Geom. **112** (2019), 199–232, with an appendix by Cristofaro-Gardiner and Keon Choi; [MR 3960266](#).
- CGFS17 D. Cristofaro-Gardiner, D. Frenkel and F. Schlenk, *Symplectic embeddings of four-dimensional ellipsoids into integral polydiscs*, Algebr. Geom. Topol. **17** (2017), 1189–1260; [MR 3623687](#).
- CGHS22 D. Cristofaro-Gardiner, R. Hind and K. Siegel, *Higher symplectic capacities and the stabilized embedding problem for integral ellipsoids*, J. Fixed Point Theory Appl. **24** (2022), Paper No. 49; [MR 4439980](#).
- EH90 I. Ekeland and H. Hofer, *Symplectic topology and Hamiltonian dynamics. II*, Math. Z. **203** (1990), 553–567; [MR 1044064](#).
- Eli91 Y. Eliashberg, *New invariants of open symplectic and contact manifolds*, J. Amer. Math. Soc. **4** (1991), 513–520; [MR 1102580](#).
- EGH00 Y. Eliashberg, A. Givental and H. Hofer, *Introduction to symplectic field theory*, Geom. Funct. Anal. **Special Volume, Part II** (2000), 560–673, GAFA 2000 (Tel Aviv, 1999); [MR 1826267](#).
- EGM18 M. Entov, Y. Ganor and C. Membrez, *Lagrangian isotopies and symplectic function theory*, Comment. Math. Helv. **93** (2018), 829–882; [MR 3880228](#).
- GH18 J. Gutt and M. Hutchings, *Symplectic capacities from positive  $S^1$ -equivariant symplectic homology*, Algebr. Geom. Topol. **18** (2018), 3537–3600; [MR 3868228](#).
- GU19 J. Gutt and M. Usher, *Symplectically knotted codimension-zero embeddings of domains in  $\mathbb{R}^4$* , Duke Math. J. **168** (2019), 2299–2363; [MR 3999447](#).
- HK20 R. Hind and E. Kerman, *J-holomorphic cylinders between ellipsoids in dimension four*, J. Symplectic Geom. **18** (2020), 1221–1245; [MR 4174300](#).
- HO20 R. Hind and E. Opshtein, *Squeezing Lagrangian tori in dimension 4*, Comment. Math. Helv. **95** (2020), 535–567; [MR 4152624](#).
- HZ21 R. Hind and J. Zhang, *The shape invariant of symplectic ellipsoids*, Preprint (2021), [arXiv:2010.02185](#).
- Hof06 H. Hofer, *A general Fredholm theory and applications* (International Press, Somerville, MA, 2006); [MR 2459290](#).
- Hut11 M. Hutchings, *Quantitative embedded contact homology*, J. Differential Geom. **88** (2011), 231–266; [MR 2838266](#).
- McD91 D. McDuff, *Blow ups and symplectic embeddings in dimension 4*, Topology **30** (1991), 409–421; [MR 1113685](#).
- McD09 D. McDuff, *Symplectic embeddings of 4-dimensional ellipsoids*, J. Topol. **2** (2009), 1–22; [MR 2499436](#).
- McD11 D. McDuff, *The Hofer conjecture on embedding symplectic ellipsoids*, J. Differential Geom. **88** (2011), 519–532; [MR 2844441](#).
- McD18 D. McDuff, *A remark on the stabilized symplectic embedding problem for ellipsoids*, Eur. J. Math. **4** (2018), 356–371; [MR 3782228](#).
- McDS12 D. McDuff and F. Schlenk, *The embedding capacity of 4-dimensional symplectic ellipsoids*, Ann. of Math. (2) **175** (2012), 1191–1282; [MR 2912705](#).

- Mül19 S. Müller, *C0-characterization of symplectic and contact embeddings and Lagrangian rigidity*, *Internat. J. Math.* **30** (2019), 1950035, 48; [MR 3995450](#).
- Ono15 K. Ono, *Some remarks on Lagrangian tori*, *J. Fixed Point Theory Appl.* **17** (2015), 221–237; [MR 3392991](#).
- Ops07 E. Opshtein, *Maximal symplectic packings in  $\mathbb{P}^2$* , *Compos. Math.* **143** (2007), 1558–1575; [MR 2371382](#).
- RS93 J. Robbin and D. Salamon, *The Maslov index for paths*, *Topology* **32** (1993), 827–844; [MR 1241874](#).
- RZ21 D. Rosen and J. Zhang, *Relative growth rate and contact Banach–Mazur distance*, *Geom. Dedicata* **215** (2021), 1–30; [MR 4330331](#).
- Sch05 F. Schlenk, *Embedding problems in symplectic geometry*, *De Gruyter Expositions in Mathematics*, vol. 40 (Walter de Gruyter, Berlin, 2005); [MR 2147307](#).
- STV18 E. Shelukhin, D. Tonkonog and R. Vianna, *Geometry of symplectic flux and Lagrangian torus fibrations*, Preprint (2018), [arXiv:1804.02044](#).
- Sie11 R. Siefring, *Intersection theory of punctured pseudoholomorphic curves*, *Geom. Topol.* **15** (2011), 2351–2457; [MR 2862160](#).
- Sie22 K. Siegel, *Computing higher symplectic capacities I*, *Int. Math. Res. Not. IMRN* **2022** (2022), 12402–12461; [MR 4466005](#).
- Sik89 J.-C. Sikorav, *Rigidité symplectique dans le cotangent de  $T^n$* , *Duke Math. J.* **59** (1989), 759–763; [MR 1046748](#).
- SYZ96 A. Strominger, S.-T. Yau and E. Zaslow, *Mirror symmetry is T-duality*, *Nuclear Phys. B* **479** (1996), 243–259; [MR 1429831](#).
- Via14 R. Vianna, *On exotic Lagrangian tori in  $\mathbb{C}\mathbb{P}^2$* , *Geom. Topol.* **18** (2014), 2419–2476; [MR 3268780](#).
- Wen10 C. Wendl, *Automatic transversality and orbifolds of punctured holomorphic curves in dimension four*, *Comment. Math. Helv.* **85** (2010), 347–407; [MR 2595183](#).

Richard Hind hind.1@nd.edu

Department of Mathematics, University of Notre Dame, Notre Dame, IN 46556, USA

Jun Zhang jzhang4518@ustc.edu.cn

The Institute of Geometry and Physics, University of Science and Technology of China,  
96 Jinzhai Road, Hefei, Anhui 230026, China

*Compositio Mathematica* is owned by the Foundation Compositio Mathematica and published by the London Mathematical Society in partnership with Cambridge University Press. All surplus income from the publication of *Compositio Mathematica* is returned to mathematics and higher education through the charitable activities of the Foundation, the London Mathematical Society and Cambridge University Press.